On the Passivity Characterization and Enforcement of Signal Power Integrity Models

A Thesis

Presented in Partial Fulfilment of the Requirements for the

Degree of Master of Science

with a

Major in Electrical Engineering

in the

College of Graduate Studies

University of Idaho

by

Nuzhat Yamin

Major Professor: Ata Zadehgol, Ph.D.

Committee Members: Brian Johnson, Ph.D., Feng Li, Ph.D.

Department Administrator: Mohsen Guizani, Ph.D.

May, 2017

Authorization to Submit Thesis

This thesis of Nuzhat Yamin, submitted for the degree of Master of Science with a major in Electrical Engineering and titled "On the Passivity Characterization and Enforcement of Signal Power Integrity Models," has been reviewed in final form. Permission, as indicated by the signatures and dates given below, is now granted to submit final copies to the College of Graduate Studies for approval.

Major Professor: _____Date_____
Ata Zadehgol, Ph.D.

Committee Members: _____Date_____
Brian Johnson, Ph.D.

_____Date_____
Feng Li, Ph.D.

Department Administrator: _____Date_____
Mohsen Guizani, Ph.D.

Abstract

In recent years, with the ever increasing operating frequencies, signal-power integrity analysis in high-speed interconnect systems is becoming increasingly important. Passivity is an integral property of such analyses, as a non-passive system may produce complexities when interfaced with other systems. Passivity needs to be verified and ensured during macromodelling of large interconnects systems. In general terms, a system is regarded as passive if it consumes energy.

Due to the importance of passivity in global systems simulation, many theories and methods addressing passivity verification and enforcement have been proposed. This thesis conducts a study of system passivity, starting from an overview of macromodeling of interconnect systems. Passivity definitions from various perspectives, conditions and requirements for passive systems and different available passivity verification and enforcement methods are presented.

In this thesis paper, four main contributions have been made: (i) we demonstrated a technique to verify passivity by realizing a 1 port system in the circuit domain, (ii) we have developed three algorithms to compute zeros from partial fraction form of rational function to assess passivity, and (iii) we develop a technique using 3-point data samples to extrapolate frequency domain response of macromodels to DC-point as a pre-processing of data before simulation of macromodels and (iv) We made a Python implementation of Second Order Arnoldi Passive Model Order Reduction (SAPOR) method. All these methods are successfully tested on several analytic and simulated examples that represent interconnect macromodeling systems to show accurate performance of the proposed techniques.

Acknowledgements

There are so many people to thank for helping me during my journey to accomplish M.Sc. degree. So many have made my stay in a new country a lot easier than I thought it was going to be. Their contributions are sincerely appreciated and gratefully acknowledged.

First and foremost I wish to thank my advisor, Professor Ata Zadehgol, director of the Applied Computational Electromagnetics and Signal Power Integrity (ACEM-SPI) Laboratory. He has been supportive since the first day I began my graduate studies at the University of Idaho. Ever since, Dr. Zadehgol has supported me not only by providing a research assistantship for more than one year, but also academically and emotionally through the rough road to finish this thesis. He helped me come up with the thesis topic and guided me over a year of development. And during the most difficult times when writing this thesis, he gave me the moral support and the freedom I needed to move on.

I would like to express my gratitude to Dr. Brian Johnson and Dr. Feng Li for being my committee members and finding out the time to be present on my defense.

I would like to acknowledge Brent Keeth, Ph.D., Sr. Fellow at Micron Technology, Inc., for support of our research in the ACEM-SPI lab.

Of course the acknowledgment would not be complete without thanking my family, who supported me throughout my entire study and encouraged my activities. This journey would not have been possible without the support and love of my parents, my brother and sister-in-law, my in-laws and last but not the least, my husband.

Thank you to all relatives, friends and my fellow colleagues of ACEM-SPI lab who in one way or another shared their support morally.

Above all, thanks to the great Almighty, for his countless mercy upon me during this whole journey.

Table of Contents

List of Tables

List of Figures

CHAPTER 1

Introduction

1.1 Research Motivation

Signal and power integrity analysis has a great impact in the design and characterization of digital circuits and communication systems. These characterizations of high-speed interconnected systems are getting increasingly dependent on reduced-order macromodelling methods [1–6]. Often these macromodels are extracted from electromagnetic simulation or from direct measurement in the form of admittance, impedance, scattering or hybrid parameters. Electrical interconnects are greatly facilitated by the rational macromodels since they can be easily converted into SPICE-compatible netlists, that allows signal and power integrity analyses using typical simulation software tools. These macromodels must be designed accurately to preserve the accurate response of the system. In macromodels, one of the most fundamental and sensitive properties is passivity. It can be easily violated during reduced-order modeling which affects circuit behavior, especially when the macromodel is interfaced with other networks. Henceforth, verification and enforcement of passivity during the derivations of macromodels have become a topic of intense research.

Noteworthy endeavors have been undertaken lately for the advancement of powerful and effective passivity verification and enforcement. Over the previous two decades, the topic of enforcing passivity has achieved significant consideration in the literature. Plenty of techniques and efforts have been demonstrated by researchers. Taking this into account, this thesis paper provides a chronicled advancement of the hypothesis relating to passivity verification and enforcement of linear systems.

This thesis concentrates on passivity verification along with enforcement. Before unfolding the contributions of this thesis in later chapters, we begin with some preliminaries about

existing passivity verification and enforcement schemes in linear systems.

1.2 Definition of Passivity

A passive system is a system that is incapable of producing energy and can consume energy only from the sources that excites it [7, 8]. Particularly, the system must absorb and accumulate energy before having the capacity to give back this energy externally. Mathematically, a system is passive if the accompanying condition is true for the combined net energy consumed by the system $x(t)$ up to any arbitrary time t [9],

$$\varepsilon_x(t) = \int_{-\infty}^{t} |x(\tau)|^2 d\tau \geq 0 \tag{1.1}$$

Furthermore, a system is denoted as strictly passive if it consumes energy, and it is passive if it does not produce energy. The specific analytical interpretation of passivity is dependent on the representation used to define the system.

1.2.1 Early Definitions

In 1954, a broad definition of passivity was proposed by Raisbeck [10] that a linear time-invariant n-port system represented by an open-circuit impedance matrix, $Z(s) = [Z_{\mu v}(s)]$, is defined as passive only if the hermitian matrix $Z(s) + Z^{*'}(s)$ is positive semi-definite in the right half-plane. An extremely thorough definition of LTI passive networks was described by Youla *et al.* in 1959 [11]. The condition for an n-port network to be passive is:

$$\int_{-\infty}^{t} \mathbf{v}^T(\tau)\mathbf{i}(\tau)d\tau \geq 0 \tag{1.2}$$

for all t and all admissible port voltages $\mathbf{v}(t)$ and currents $\mathbf{i}(t)$. This equation is valid for impedance or admittance representation.

The definition of passivity is similar for scattering representation, [11] which is as follows,

$$\int_{-\infty}^{t} [a^T(\tau)a(\tau) - b^T(\tau)b(\tau)]d\tau \geq 0 \tag{1.3}$$

where $a(t)$ and $b(t)$ are the incident and reflected power waves at the ports respectively. These definitions are valid for lumped and distributed systems alike.

In 1966, Resh [12] and Kuo [13] presented the Raisbeck proposition with a slight modification. In 1969, Wohlers [9] gave explicit validation using the theory of distribution. The aforementioned definition has two noteworthy shortcomings. There might not be any state that stores zero energy, or there might be multiple states having zero energy stored in case of a nonlinear network. Additionally, the network could portray non-passive properties when it is initiated in a state where (1.2) is invalid.

To overcome the above problems, a new theory by Wyatt et al. [14] defined passivity in analog systems that are also nonlinear. This definition shapes the premise for a generalized nonlinear definition of passivity for digital networks. Chua et al. defines passivity in [15] that the voltage current pairs $\{\mathbf{v}(t), \mathbf{i}(t)\}$ are called admissible if

$$\int_{a}^{b} |\langle \mathbf{v}(t)\mathbf{i}(t)\rangle| dt < +\infty \tag{1.4}$$

for all real a and b. A network is passive if there exists a real-valued function E of the initial state x_0 such that

$$\int_{0}^{T} |\langle \mathbf{v}(t)\mathbf{i}(t)\rangle| dt + E(o_0) \geq 0 \tag{1.5}$$

for all admissible pairs $\{\mathbf{v}(t), \mathbf{i}(t)\}$, all $T \geq 0$ and all initial states x_0

1.2.2 Laplace Domain Definition

In the Laplace domain, passivity of a system is interconnected with two important concepts, Positive realness and Bounded Realness. A system represented with immittance matrix is passive if the corresponding transfer function is positive-real. A transfer matrix $H(s)$ represents a passive linear system if it meets the following conditions [9]:

1) each element of $H(s)$ is defined and analytic in $\Re e(s) > 0$;

2) $H^H(s) + H(s) > 0$ for all s such that $\Re e(s) > 0$:

3) $H(s^*) = H^*(s)$

For systems with scattering matrix representation, passivity depends on the bounded-realness of the transfer function. A transfer matrix $H(s)$ represents a passive linear system if and only if

1) each element of $H(s)$ is defined and analytic in $\Re e(s) > 0$;

2) $I - H^H(s)H(s) > 0$ for all s such that $\Re e(s) > 0$:

3) $H(s^*) = H^*(s)$

The superscripts H and $*$ denote transpose conjugate and the complex conjugate, respectively.

From the presumption of strict stability, poles are not permitted on the imaginary axis for the scattering form of system, and condition (1) has to be valid for $\Re e(s) > 0$. Although conditions (1) and (3) are easy to fulfill, satisfaction of condition (2) poses serious numerical difficulties. This fact roused critical research endeavors in the most recent years, aiming at the realization of quick and strong calculations for passivity verification and enforcement models.

1.3 Passive Macromodelling

Building a reduced-complexity behavioral description of a device or a system of devices retaining the significant property of passivity is referred to as Passive Macromodelling. Pas-

sivity Verification and Enforcement methods consist of two primary approches, a) Passive Macromodelling and b) a two-stage process that first recognizes an underlying model, and after that enforces passivity through an appropriate perturbation process. These two approaches have been illustrated in Figures 1.1 and 1.2 respectively. In this section, we have discussed about the most common passive macromodelling techniques.

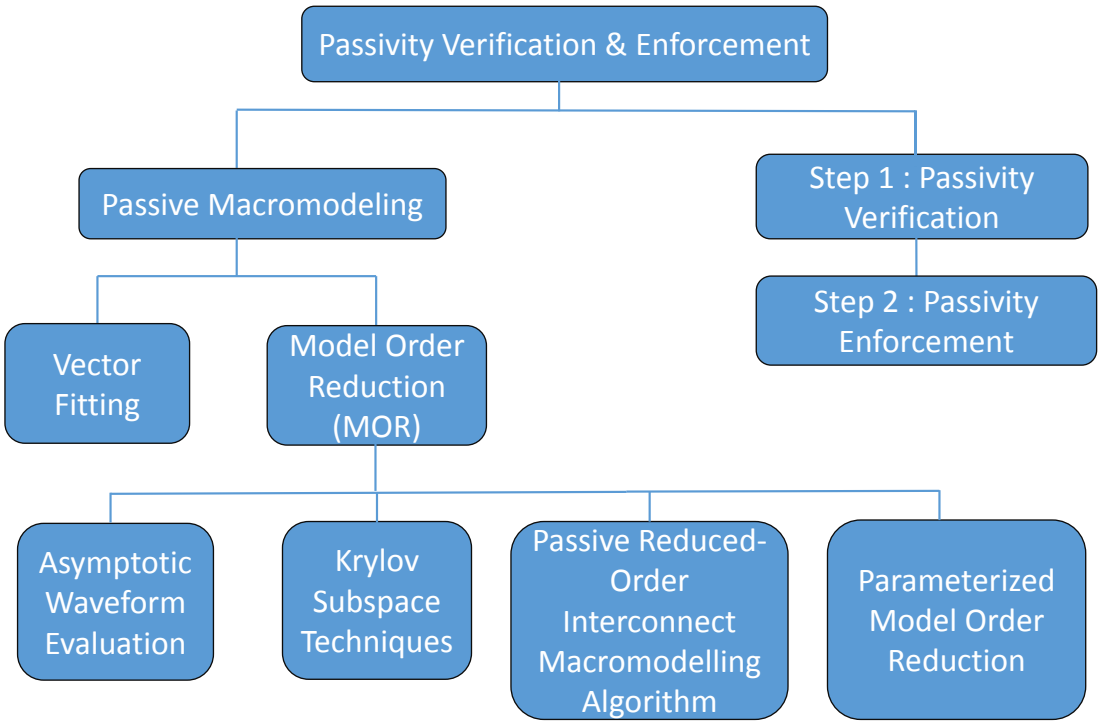

Figure 1.1: Passive Macromodelling Techniques

1.3.1 Model Order Reduction Techniques

Model order reduction (MOR) techniques fulfill the requirement for accurate, downsized, compact models [16]. These models are combined to form an approximate yet detailed representation of the whole system. Starting with a number of ODEs, MOR techniques produce confirmed passive reduced-order models. Projection or truncation processes are used to obtained compressed models. With the ever-increasing scale of circuits and efforts to decrease the order of system magnitude, the traditional model order reduction (MOR) approach preserves fundamental system properties like passivity. The most notable model order reduction techniques include Padé Approximation [17] and AWE [18], Complex Frequency Hopping, Krylov subspaces [19, 20], the Arnoldi process and PRIMA.

Asymptotic Waveform Evaluation:

Padé approximation based reduced order modeling schemes have been identified to be effective measures for different modelling and simulation techniques. The asymptotic waveform evaluation (AWE) [21] was one of the first Padé based schemes. The basis for this technique is moment matching. When the Padé approximation based model order reduction technique is used in dynamic models, it does not preserve the passivity. A few unstable zeros and poles cause this non-passivity. A distinct passive model of reduced order can then be achieved by implying some stable zeros and poles by retaining the estimation property of the Padé approximant as much possible.

Krylov Subspace Techniques:

The Krylov subspace block is another projection technique for the estimation of multi-port system models of reduced order. We can define a Krylov subspace as a series of vectors

produced by a predefined matrix and a vector in following equation (1.6).

$$K_n(A, r) = span\{r, Ar, A^2r, ..., A^{n-1}r\} \tag{1.6}$$

where A is a matrix, r initial vector, the n^{th} Krylov subspace $K_n(A, r)$ is a sequence of n column vectors. Half as many moments are matched by Krylov subspace models compared to Padé approximation based models and these models are always passive. Another well-known Krylov-subspace algorithm is the Arnoldi process [22]. Arnoldi based models are not characterized by Padé approximation, and accordingly, all in all, the accuracy is not as precise as a Padé based model of equal order.

Passive Reduced Order Interconnect Macromodelling Algorithm (PRIMA):

Passive Reduced Order Interconnect Macromodelling Algorithm or PRIMA is an Arnoldi based reduction process. In [23], it has been established that PRIMA preserves passivity of reduced order models for typical RLC circuits. A block interpretation of the Arnoldi process is first utilized by PRIMA and then reduced order models are obtained by mapping the matrices. These matrices mapped onto the Arnoldi basis vectors represent the RLC transfer function. The fact that PRIMA ensures the passivity is proved by experimental results which is important for time domain analyses.

Parameterized Model Order Reduction:

The variation-induced issues are recognized by Parametric MOR or variational MOR [24] (VMOR) techniques in circuit and system modeling. Typical cases are geometric variations [25] and process uncertainty [26]. PMOR is valid for both linear and nonlinear systems. [27] proposes a unique parameterized model order reduction technique which produces parametric downsized models. A powerful and steady sequence of passivity preserving MOR

method ensures the global passivity of the parametric reduced order model. A domain of positive interpolation operators are the basis for the sequence of MOR methods. The PMOR algorithm retains the three conditions mentioned in section 1.2.2 over the unified design space.

PMOR methods ensure the passivity of systems when the original behavioral depiction of the circuit is passive. But the problem associated with it is the unavailability of such a behavioral model (circuit). Hence, different attempts have been undertaken for the characterization of macromodels in time or frequency domain. Despite providing very precise estimation, the general output of such methods is not always a passive model.

1.3.2 Vector Fitting

One of the most successful approaches for extracting macromodels of linear interconnects and LTI systems, is achieved by applying frequency domain fitting techniques to measured or simulated data in the frequency domain [28–33]. The first approximation is made via a rational function. Followed by an equivalent circuit or synthesis of a state space form to facilitate simulation with a circuit simulator. A fascinating development in passive macromodelling occurred in the late 1990s when the vector fitting (VF) algorithm was first introduced. Since its first introduction [28], it has emerged as a widely used technique for macromodel generation from frequency domain data obtained via measurement or simulation. We can obtain reduced order state space macromodels by rational curve fitting algorithms [28–33] from frequency-domain responses presented by scattering, admittance, or impedance matrices; with a view to identifying dominant pole-residue pairs expressed in a partial fraction form. The poles and residues are selected such that the resultant fitted transfer function becomes passive. Thus, it is possible to approximate the tabulated transfer function via a summation of rational functions with complex poles $p_1, p_2, \ldots, p_n$ and complex residues $q_1, q_2, \ldots, q_n$:

$$H(\jmath\omega) \approx \sum_{i=1}^{n} \frac{q_i}{\jmath\omega - p_i} \tag{1.7}$$

The algorithm of vector fitting developed in [28] produce one possible technique to provide such a representation. The associating impulse response can be obtained analytically and can be expressed as the following sum:

$$H(t) \approx \sum_{i=1}^{n} q_i e^{p_i t} \tag{1.8}$$

Beyond the measurement frequency bandwidth, where there is no fitting restriction as well a minimal errors in the frequency-domain data may end up in generating a non-passive model. Therefore, vector fitting does not always ensure passivity of the rational approximated macromodel generated through it. Under the circumstance, substantial research effort has been given to ensure passivity, and different enforcement techniques in literature can be utilized to serve the purpose.

1.3.3 Loewner matrix Interpolation

Loewner matrix (LM) interpolation is a very recent macromodelling technique mentioned in [34]. It is able to display great scaling in the number of ports and poles for both lumped [35, 36] and distributed [37–39] networks. This technique facilitates use by generating a macromodel directly in the descriptor state space system (DS) framework directly. And the method retains passivity very accurately in a system of increasing order. As a matter of fact, producing a reduced order macromodel at the expense of minimization in preciseness is valuable.

1.4 Existing Passivity Verification Techniques

A system is passive when the total energy entering into a system is non-negative throughout time. This definition implies a specific interpretation of passivity related to the system transfer function. The implication on the transfer function is outlined for general linear time-invariant (LTI) systems in that it has to be Positive Real for immittance representations and

Bounded Real for scattering representations. We shed light into these passivity constraints for state space representation of the system in the accompanying sections. These conditions will lead to some useful passivity verification and enforcement schemes for interconnect systems. Figure 1.2 illustrates a number of passivity verification and enforcement techniques. The classical method of passivity verification for macromodels is done by sweeping frequency along eigenvalues of the real part of the admittance matrix. However, this methodology experiences a few disadvantages, for example, the maximum frequency and the range of the sweep has to be precise for accurate outcome. Likewise, it fails to distinguish the precise areas of violation.

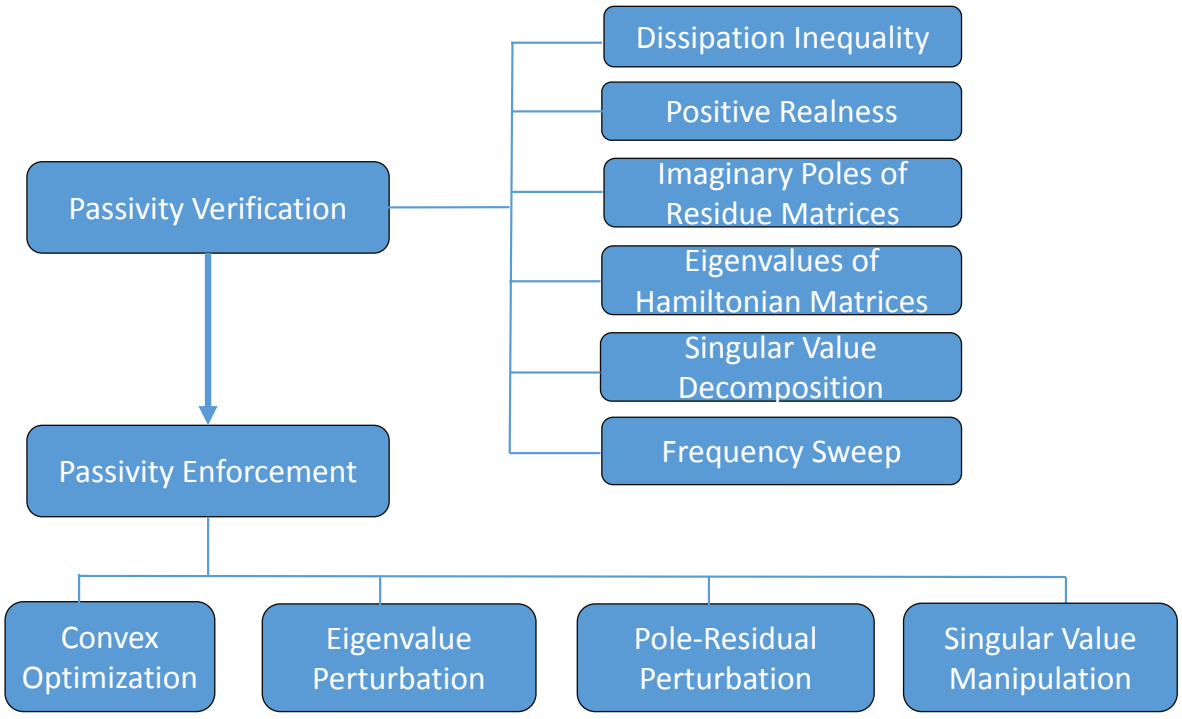

Figure 1.2: Passivity Verification and Enforcement Techniques

1.4.1 Linear Matrix Inequality

Positive/bounded realness described in 1.2.2 forms the basis of the Linear Matrix Inequality based passivity verification technique, which makes passivity of a system related to the transfer function. $H(s)$ is passive if and only if the following linear matrix inequality (LMI) are satisfied.

$$\begin{bmatrix} -A^tP - PA & -PB + C^t \\ -B^tP + C & (D + D^t) \end{bmatrix} \geq 0 \tag{1.9}$$

with $P = P^T \geq 0$. And the Bounded Real Lemma, i.e,

$$\begin{bmatrix} -A^tP + PA & PB & C^t \\ B^tP & -I & D^t \\ C & D & -I \end{bmatrix} \leq 0 \tag{1.10}$$

with $P = P^T \geq 0$. We can assess the passivity of immitance systems by a) checking the (Hermitian) symmetry and nonnegative definiteness of the residue matrices from the purely imaginary poles (including $s = 0$ and $s = \infty$); b) taking the state space representation of the system and checking their positive realness.

1.4.2 Hamiltonian Matrices

We can verify the passivity of a transfer function in any of the state space forms (scattering, impedance, admittance or hybrid) by spectral properties of Hamiltonian matrices. Checking the presence of purely imaginary eigenvalues in the corresponding Hamiltonian matrix is a general test for passivity [40]. If there are one or more purely imaginary eigenvalues found, the system is considered non-passive. The state–space system is passive if there are no imaginary eigenvalues in the corresponding Hamiltonian matrix [41] given by equation (1.11):

$$M = \begin{bmatrix} A - B(D + D^t)^{-1}C & B(D + D^t)^{-1}B^t \\ -C^t(D + D^t)^{-1}C & -A^t + C^t(D + D^t)^{-1}B^t \end{bmatrix} \tag{1.11}$$

The formulation of this technique using a Hamiltonian matrix, being independent of frequency – is the main advantage. Hence, the absence of imaginary eigenvalues inherently suggests that the associated macromodel is passive. Here, we present an example to validate this technique to verify the passivity of a system. We consider one passive and one non-passive system described by the state space representation $\{A, B, C, D\}$. The Hamiltonian matrix of the non-passive system exhibits purely imaginary eigenvalue which is verified by the largest singular value of the transfer matrix. The singular value is greater than 1 for all frequencies for the non-passive system. The validation of this method has been illustrated in Figure 1.3.

It is absolutely necessary to know the frequency locations accurately for which the real part of the eigenvalues turn from positive to negative, if we require a faster passivity enforcement. Conventionally, frequency regions that have violations have detected eigenvalues of Hamiltonian matrix M that is associated with the state space model [6,42,43]. When $D+D^t$ is a positive definite matrix, the real part of the symmetric admittance matrix $F(\jmath(\omega_0))$ is singular if $\jmath\omega_0$ is an eigenvalue of the associated Hamiltonian matrix M. We can infer from this statement that a purely imaginary eigenvalue of the Hamiltonian matrix M detects the frequency at which $F(\jmath\omega)$ is singular (i.e., the macromodel becomes non-passive).

1.4.3 Singular Value Decomposition Method

In the novel work by Campbell et al., a different approach for verifying passivity by applying singular value decomposition of the S-matrix is demonstrated [44]. The macromodeling can be expressed as:

$$H(s) \approx \frac{N(s)}{D(s)} = \sum_{n=1}^{N} \frac{c_n}{s - \alpha_n} + d \tag{1.12}$$

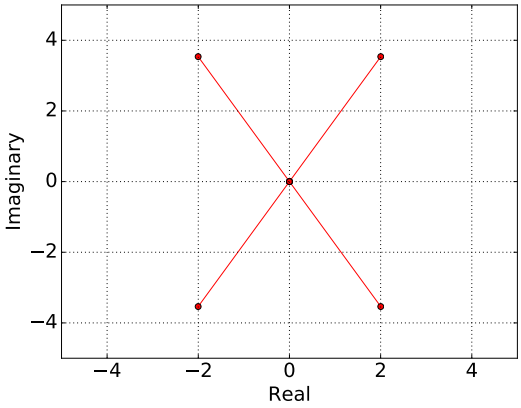

(a) Hamiltonian Matrix Eigenvalue of Passive system

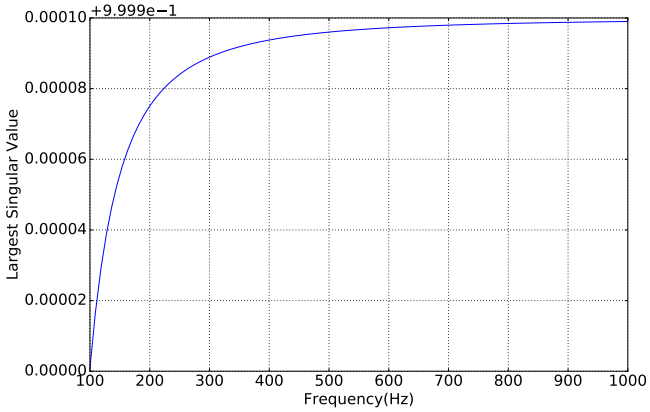

(b) Largest Singular value of Passive system

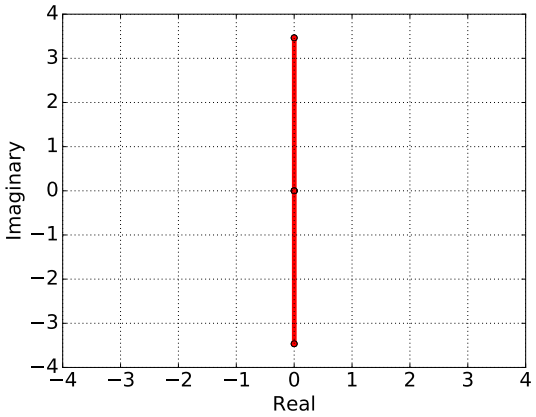

(c) Hamiltonian Matrix Eigenvalue of Non-Passive system

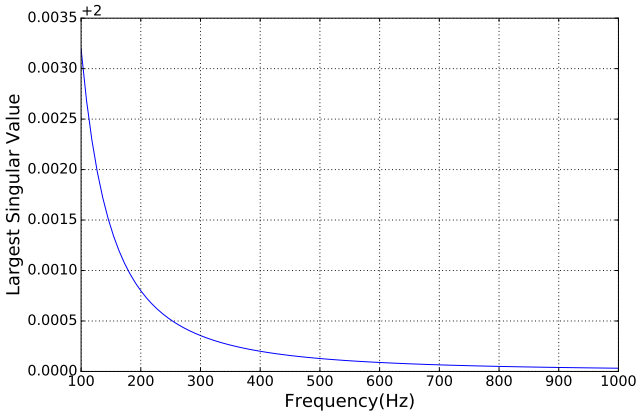

(d) Largest Singular value of Non-Passive system

Figure 1.3: Validation of using Eigenvalues of Hamiltonian Matrices to verify Passivity.

where $H(s)$ is the transfer function of the system, c_n is the n^{th} residue and α_n is the n_{th} pole. The system can be represented in the state space form, followed by a curve fitting process, as follows

$$\begin{aligned} \dot{x}(t) &= A.x(t) + B.u(t) \\ y(t) &= C.x(t) + D.u(t) \end{aligned} \tag{1.13}$$

where, $A \in \mathbb{R}^{n\times n}$, $B \in \mathbb{R}^{n\times m}$, $C \in \mathbb{R}^{m\times n}$, $D \in \mathbb{R}^{m\times m}$ are the system, input, output and feed-forward matrices respectively. Moreover, $x \in \mathbb{R}^n$ is the state , $u \in \mathbb{R}^m$ is the input and $y \in \mathbb{R}^m$ is the output of the system, respectively and $\frac{d}{dt}x(t)$ is denoted by $\dot{x}$. The system transfer function of the system can be rewritten as follows:

$$H(s) = C.(sI - A)^{-1}B + D \tag{1.14}$$

Here, s is the Laplace variable, $s = \jmath\omega$ and ω is the angular frequency in (rad/sec). The condition for the system to be passive requires that the Hermitian matrix associated with the $H(s)$ be non-negative definite and unitary, so that the norm of the S-matrix has to be less than or equal to 1, that is, $\| S(\jmath\omega) \|_2 \leq 1$. This implies that the maximum singular value of S has to be less than or equal to 1 for all frequency ω, for the passivity criterion to hold. Mathematically, we can express it as:

$$\max_{i,\jmath\omega} \sigma_i \leq 1 \quad \forall\sigma_i(\jmath\omega \in \sigma(S(\jmath\omega)) \quad \forall\omega \tag{1.15}$$

Where σ denotes the singular values of $H(\jmath\omega)$. The system will be passive if and only if these singular values, σ are less than or equal to one.

1.4.4 Frequency Sweeping

The frequency sweeping method is another convinient way to check passivity. In [45], a frequency sweeiping method has been proposed which is called the reciprocal frequency

sweeping. It checks passivity by dividing the frequency axis into its original and reciprocal segments by the largest frequency f_{max} of the S-matrix, then sweeps the two parts individually. This method is based on the bounded real lemma. Frequency sweeping method described in [46] is to check the positive (or bounded) realness of H(s) at a set of sampling points $s = \jmath\omega_k (k = 1, 2, ...)$ along the imaginary axis. The concept is basic, yet the calculations are not dependable. Despite adaptive sampling and a reciprocal sampling methods that have been discussed in [46] and [45] respectively, some regions show non-passivity in the vicinity of sampling points and passivity can not be accurately verified by finite sampling. In [47], two sweeping methods have been proposed for checking passivity of descriptor systems: extended reciprocal sweeping method and unit circle sweeping method. Frequency sweeping methods are very efficient in terms of accuracy and locating passivity violations, which makes consecutive procedures easier.

1.4.5 Generelized Hamiltonian Pencil

Compared with the standard state space equivalents, passivity tests of descriptor system (DS) are explored much less. In [48], we find a new method for passivity test of descriptor systems (DSs) called the generalized Hamiltonian method (GHM). For any system basis, this method is capable of testing passivity of Descriptor systems without nominal realization. This is a frequency-independent method and requires less time in system disintegration. Also, GHM works well where Hamiltonian method fails, and it identifies passivity violations more accurately than frequency sweeping techniques. Furthermore, the GHM method of passivity test has been expanded for immittance Descriptor systems [49] and S-parameter descriptor systems [50].

1.5 Existing Passivity Enforcement Techniques

Passive macromodeling techniques grew very rapidly based on several published technical papers on passivity enforcement. The exertion of passivity enforcement is more challenging than curve fitting. Passivity can be enforced by implying the conditions using a number of different methods. These imply a relation between the passivity conditions and the elements of the transfer function and state space representation, individually. Hence, passivity enforcement schemes involve more numerical complexities than the complexities involving rational curve fitting techniques. In addition, since ensuring passivity includes more constraints than any other fundamental properties of systems, it is necessary to take care of the potential loss of accuracy cautiously. These constraints gave rise to noteworthy research attempts in the past few years. Existing passivity enforcement methods include convex optimization methods [51], Eigenvalue Perturbation Method [42,46,52], Frequency Pole-Residual Perturbation [53–56], Singular Value Manipulation [44] and Local compensation [57].

1.5.1 Convex Optimization Method

Passivity enforcement using convex formulation introduced in reference [58] is described on the basis of Linear Matrix Inequality (LMI) [41] conditions. Unfortunately, this method is not computationally effective, that is it requires more memory to run in practical situations. Convex formulation guarantees the passivity of the system matrix with the least modification. Additionally, it requires a very small number of operations and the modified system is precisely accurate. But the main disadvantage of this method is the substantial measure of computation required for the algorithm. The number of variables is $N(N+1)/2 + NP$. If we assume that the number of states N is larger by a large margin than the number of ports P, then the leading term is in the order of $O(N^2)$. Typically, the total expenditure for determining an LMI optimization is in the order of $O(K^3)$. Therefore, the resulting cost in this technique approximately becomes $O(N^6)$. Other than small-scale models that have

a small number of states, this formulation is incapable of handling most systems. More recently, advancement on the convex optimization scheme [59] has shown that it is possible to obtain the passive macromodel in a limited number of iterations within a satisfactory level of preciseness.

1.5.2 Eigenvalue Perturbation Method

The eigenvalue perturbation method falls into the class of spectral perturbation of reasonably characterized Hamiltonian matrices. Specific identification of passivity violations is possible through a Hamiltonian matrix from its imaginary eigenvalues which are derived from the state space model. But since the matrix size is equivalent to twice the number of model states, the numerical extraction of eigenvalues require more time for larger models. Thus, transformation of large scale macromodels may turn out to be very demanding. Recent developments [60–62] have reduced the Hamiltonian matrices to half of their actual size for passivity verification. The half size test matrices reduces the computational cost by a factor of eight. But it can only be derived in case of symmetric singular matrices. Another shortcoming of this method is convergence as it is based on non-convex formulation. In [63–65], different approaches have been applied to make the eigenvalue method more effective. More recent work [66] on eigenvalue perturbation presents an inverse eigenvalue method. It is an advanced iterative method to ensure passivity in admittance matrices associated with a system.

1.5.3 Pole-Residual Perturbation Method

Pole-Residual perturbation is the method in which we can enforce passivity by perturbing poles/residues. The first class of such methods are perturbation of the residue matrix to make required modification to the system to ensure passivity which are described in [53–55]. In [54, 55], the perturbation has been applied to the whole residue matrix. In [56], poles are modified to enforce passivity but the perturbation has been applied individually at each pole.

These methods are not globally optimum. However, [67] proposed an innovative passivity enforcement method which changes both zeros and poles in steps of iteration while explicitly keeping the error level minimum at each iteration step.

1.5.4 Singular Value Manipulation

Macromodels based on S-parameters have an implication on the singular values in the frequency domain that they have to be unitary bounded for the model to be passive. So, another way of restoring passivity is to manipulate the singular values to make it less than unity at all frequencies. The authors in [68] present an enforcement method that searches for the minimum perturbations needed for passive realization.

Some other passivity enforcement is based on schemes assuming that the macromodel is strictly stable. This technique ensures the explicit enforcement of the passivity conditions at some precisely chosen frequency points that confers to assert condition (2) as

$$\min \lambda\{\Phi(\jmath\omega)\} \geq 0, \ \forall\omega \tag{1.16}$$

Equation (1.16) is characterized at an accurately specified collection of distinct frequency samples. The modification of singular value is executed at the frequencies that do not satisfy equation (1.16), directing toward eliminating passivity violations and reinforce passivity globally.

1.5.5 Recent Advancement on Enforcement

Very recent developments [69–75] include more advanced techniques of passivity enforcement, i.e, passive macromodeling method that results in close-to-band (CTB) violations [70] by extending frequency samples efficiently, sensitivity-weighted passivity enforcement method [71] especially for Power Distribution Networks (PDN). In [72, 73], the author presents two enforcement methods based on localization. These methods cut down the memory as well

as computation time by a significant order in comparison to Bounded Real Lemma based convex formulations. In contrast with the conventional passivity enforcement schemes, [74] comes up with a data pre-processing approach to reduce data passivity violations before model extraction followed by passivity enforcement, working towards an accurate model interpretation. On the other hand, a post-enforcement optimization technique is proposed in [75]. This technique takes a passive model which is not so accurate as the initial point, and searches locally in order to find the local optimum.

1.6 Thesis Contribution

The main contributions focus on Passivity Verification and Enforcement. The work proposed in this thesis can be summarized as follows:

1. A passivity verification and enforcement technique has been proposed based on system poles and residues. This method also successfully determines the passivity violation frequencies. This methods enforces passivity by minimally changing the magnitude of the frequency response. A future topic of work can be to enforce passivity minimally changing the magnitude response as well as the phase of frequency response.

2. Since passivity can be verified by looking at the location of the system zeros at the Laplace-plane, we have also proposed some more passivity verification techniques based on computing the zeros by finding the local minima in the s-plane. We first develop an algorithm to compute the real zeros. This method is then further developed for identifying the complex zeros by searching the 2-dimensional Laplace s-plane for local minima. This method has been improved more to distinguish the zeros if the system suffers from noise. The improved algorithm computes the system zeros successfully from noise affected data.

3. Modern frequency domain measurement equipment cannot simultaneously cover high and low frequency ranges with good resolution and accuracy. Therefore, it becomes critical to extrapolate the data into the DC region before using it in the simulations. In this thesis, we also develop a technique to extrapolate frequency domain response of macromodels to

DC-point using 3-point data samples.

4. With increased range of frequencies, we constantly need to make compact behavioral models from large scale circuits. Model Order Reduction is a great technique to fulfill this need along with preserving the fundamental properties like passivity of the system. In this thesis, we have implemented a Second Order Arnoldi based Passive Model Order Reduction (SAPOR) [76] method in the python programming language. This method preserves the passivity of the system by generating an orthogonal projection matrix. By projecting this matrix on our sample system, we reduce the system by a large order. We have presented some numerical examples to validate these results.

CHAPTER 2

Verification and Enforcement of Passivity through Direct Minimal Modification of Equivalent Circuits

The passivity verification and enforcement method described in this chapter has been published in the conference paper entitled "Verification and Enforcement of Passivity through Direct Minimal Modification of Equivalent Circuits", IEEE EMC Europe 2016 Wroclaw International Symposium and Exhibition on Electromagnetic Compatibility, Wroclaw, Poland, Pages: 756 - 759.

2.1 Introduction

The multiport scattering (S-) parameter matrix is greatly utilized in describing circuit modeling with interconnect systems with broadband characteristics to perform signal-integrity and power-integrity simulations accurately [77]. The S-parameters can be obtained either directly from measurements or from rigorous full-wave electromagnetic simulation [78]. But the difficulty is that the measurement errors or the numerical errors associated with the electromagnetic analysis tools may cause the data to be non-passive in the frequency bandwidth of interest [78]. But, the passivity of the S-parameter data is important for macro modeling the interconnect system and ensuring an accurate global system.

Hence, it is highly desired that the tabulated S-parameter data is verified for passivity in the bandwidth of interest, prior to its circuit compatible modeling [78]. Poles and residues can be obtained by vector fitting method [78] and the partial fraction form of the rational transfer function can be used in realizing the single port system by equivalent circuit synthesis. The objective of our work is to verify passivity of S-parameter tabulated data to accomplish the above. In this chapter, a new method has been proposed for passivity verification and determination of any passivity violation frequencies. It also develops an algorithm to enforce

passivity of the system.

The remainder of this chapter is organized as follows. Section 2.2 describes the problem formulation and discuss the proposed passivity verification and enforcement algorithm, respectively. Section 2.3 and 2.4 present numerical results and summary, respectively.

2.2 Formulation

2.2.1 Equivalent Circuit Synthesis

Linear single-port (and multi-port) networks can be characterized by the partial fraction form of transfer function. Poles and residues in the partial fraction form can be realized into equivalent impedance branches through the cellular approach describing in [77]. For real poles and residues, a system transfer function can be characterized by the partial fraction form.

$$H(s) = \sum_{n=1}^{N} \frac{c_n}{s - p_n} \tag{2.1}$$

where c_n is the n^{th} residue, and p_n is the n^{th} pole. For complex-conjugate pair of poles and residues,

$$H(s) = \sum_{n=1}^{N} \frac{c_n}{s - p_n} + \frac{c_n^*}{s - p_n^*} \tag{2.2}$$

These poles and residues can be realized into equivalent circuit branches by the transformation used in [77]. For real poles and residues:

$$R = \frac{-p}{c} \qquad , \qquad L = \frac{1}{c} \tag{2.3}$$

where R is the equivalent branch resistance and L is the equivalent branch impedance and

we get the branch impedance as a series connection of R and L:

$$Z(\omega) = R + j\omega L \tag{2.4}$$

For complex conjugate pair of poles and residues, the transformation [77] is:

$$\begin{aligned} R_a &= \frac{c_i p_i - c_r p_r}{2c_r^2} \quad , \quad R_b = -\frac{p_i^2(c_i^2 + c_r^2)}{c_i p_i + c_r p_r} \\ L &= \frac{1}{2c_r} \quad , \quad C = \frac{2c_r^3}{p_i^2(c_i^2 + c_r^2)} \end{aligned} \tag{2.5}$$

where R_a, L, R_b and C are the equivalent series resistance, inductance and shunt resistance and capacitance. We can represent the macro model [79] as a series connection of R_a, L and R_b, C connected in parallel together. So, we get the impedance of a branch for each frequency ω as

$$Z(\omega) = R_a + j\omega L + (\frac{1}{R_b} + j\omega C)^{-1} \tag{2.6}$$

The individual RLRC branches corresponding to each partial fraction term are connected in parallel and the total impedance of the whole system for each frequency is given by:

$$Z_T(\omega) = \frac{1}{\sum_1^m \frac{1}{Z(\omega)}} \tag{2.7}$$

where m denotes the number of branches.

2.2.2 Passivity Verification

The definition of a passive system model characterized by an impedance matrix implies that the impedance matrix has to be bounded real since it is unable to generate energy. A single-port impedance $Z(\omega)$ is passive when the real part of $Z(\omega)$ is passive at all frequency,

$$Re\{Z(\omega)\} \leq 0 \quad \forall\, \omega \in \mathbb{R} \tag{2.8}$$

2.2.3 Passivity Enforcement

Let us consider an impedance matrix of a single port system synthesized by partial fraction of rational function. If the total impedance is non-passive at any given frequency, then we add a resistance R' to its non-passive branches in series to enforce passivity. In order to keep the change of impedance transfer function minimal, we add an imaginary element R'_i in series with the branch to compensate the change in the real part of impedance so that the magnitude of impedance remains the same. The imaginary series element can be called an imaginary resistance. These elements are given by,

$$R' = -1.01(Re\{Z_m(\omega)\}) \tag{2.9}$$

where m is the branch indice. For RL branches, the imaginary resistance is set to,

$$R'_i = -\omega L + \sqrt{\omega^2 L^2 - (2RR' + R'^2)} \tag{2.10}$$

and for RLRC branches, the imaginary resistance is set to,

$$\begin{aligned} R'_i = &-\omega L + \frac{CR_b^2\omega}{1 + C^2R_b^2\omega^2} \\ &+ \frac{1}{2}\sqrt{2\omega L - \frac{2CR_b^2\omega}{1 + C^2R_b^2\omega^2} - 4R'\big(R' + 2(R_a + \frac{R_b}{1 + C^2R_b^2\omega^2})\big)} \end{aligned} \tag{2.11}$$

R'_i has been chosen as such the magnitude response remains minimally changed.
So, the modified RL branch impedance becomes,

$$Z'(\omega) = R_a + j\omega L + R' + jR'_i \tag{2.12}$$

and the modified RLRC branch impedance becomes,

$$Z'(\omega) = R_a + j\omega L + (\frac{1}{R_b} + j\omega C)^{-1} + R' + jR'_i \tag{2.13}$$

2.3 Numerical Results

In the following we show an approach for passivity enforcement, based on the method developed in Section 2.2. We used 18 sets of poles and residues (real and complex-conjugate pair) described in [28] and got 2 RL branches for real poles and residues and 8 RLRC branches for complex-conjugate pairs of poles and residues. When the total impedance is negative at any frequency, we add R' to its non-passive branches at that frequency. After enforcement, we observe that the whole system has become passive for all frequencies. The magnitude of each branch impedance (before and after adding R') has been plotted against frequency ranging from 0.1 to 0.1GHz in Figure 2.2 and Figure 2.3.

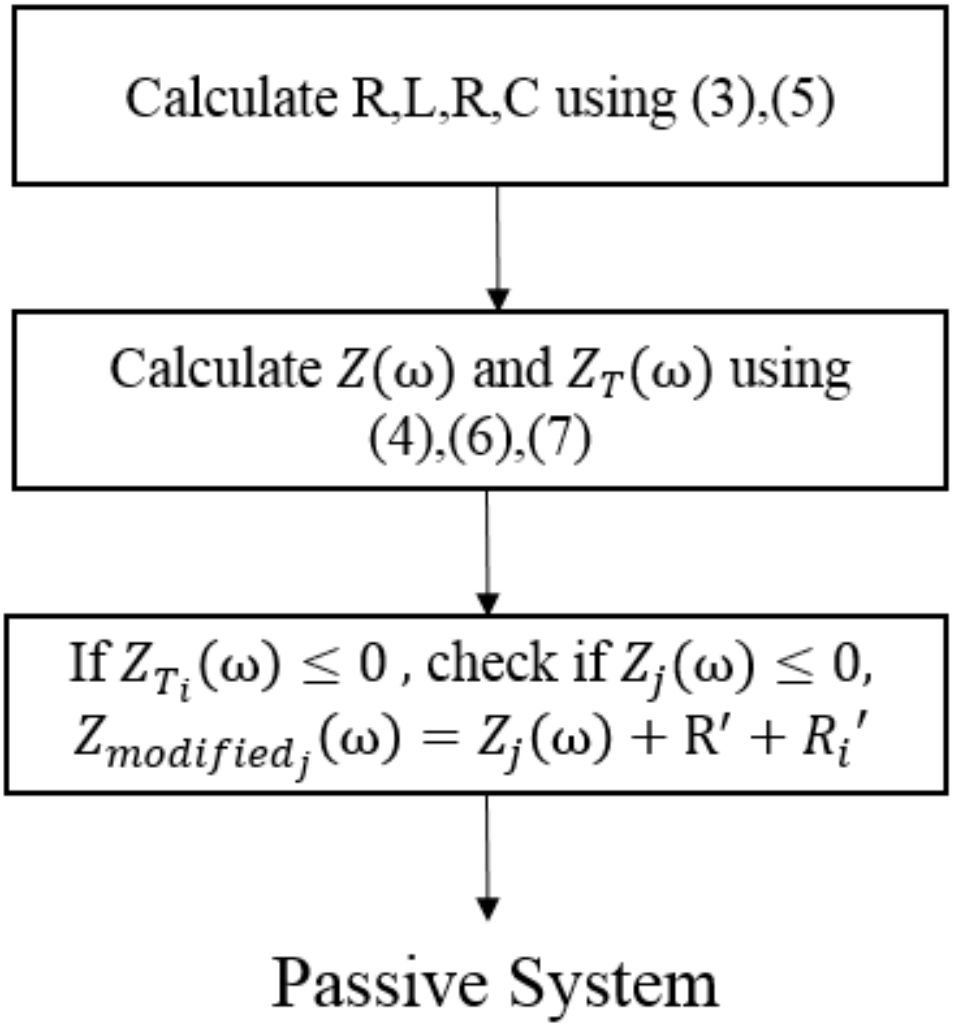

Figure 2.1: Passivity Enforcement Algorithm. (Source: Nuzhat Yamin, Ata Zadehgol, Verification and enforcement of passivity through direct minimal modification of equivalent circuits. Copyright ©2016, IEEE International Symposium on Electromagnetic Compatibility-EMC EUROPE)

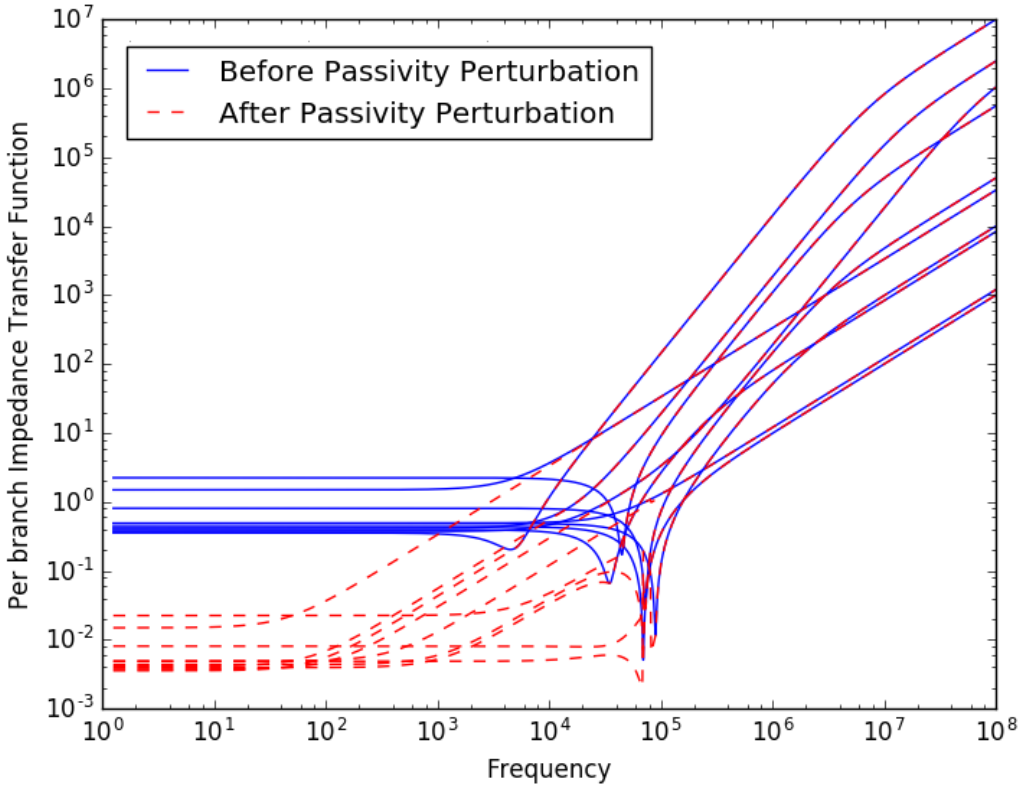

Figure 2.2: Frequency vs Magnitude of Branch Impedance plot. (Source: Nuzhat Yamin, Ata Zadehgol, Verification and enforcement of passivity through direct minimal modification of equivalent circuits. Copyright ©2016, IEEE International Symposium on Electromagnetic Compatibility-EMC EUROPE)

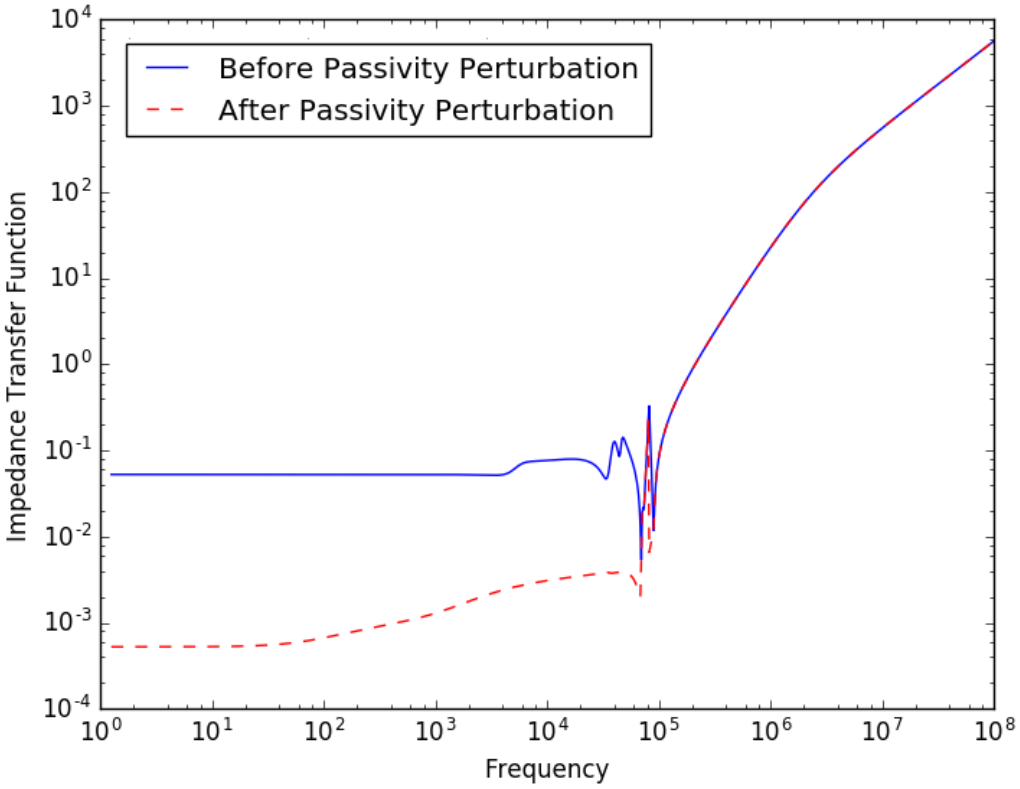

Figure 2.3: Frequency vs Magnitude of Total Impedance plot. (Source: Nuzhat Yamin, Ata Zadehgol, Verification and enforcement of passivity through direct minimal modification of equivalent circuits. Copyright ©2016, IEEE International Symposium on Electromagnetic Compatibility-EMC EUROPE)

But the magnitude response looks too deviated in the non-passive regions. The absolute error plot is shown in Figure 2.4. The error function is given by,

$$Error(\omega) = |Z(\omega) - Z'(\omega)| \tag{2.14}$$

In order to compensate this change and keep the magnitude response minimally changed, we add Ri' in series with the non-passive branch impedance at the non-passive frequencies and we find a very good match shown in Figure 2.5, Figure 2.6 and Figure 2.7. The value of Ri' has been set such that equation (2.15) holds.

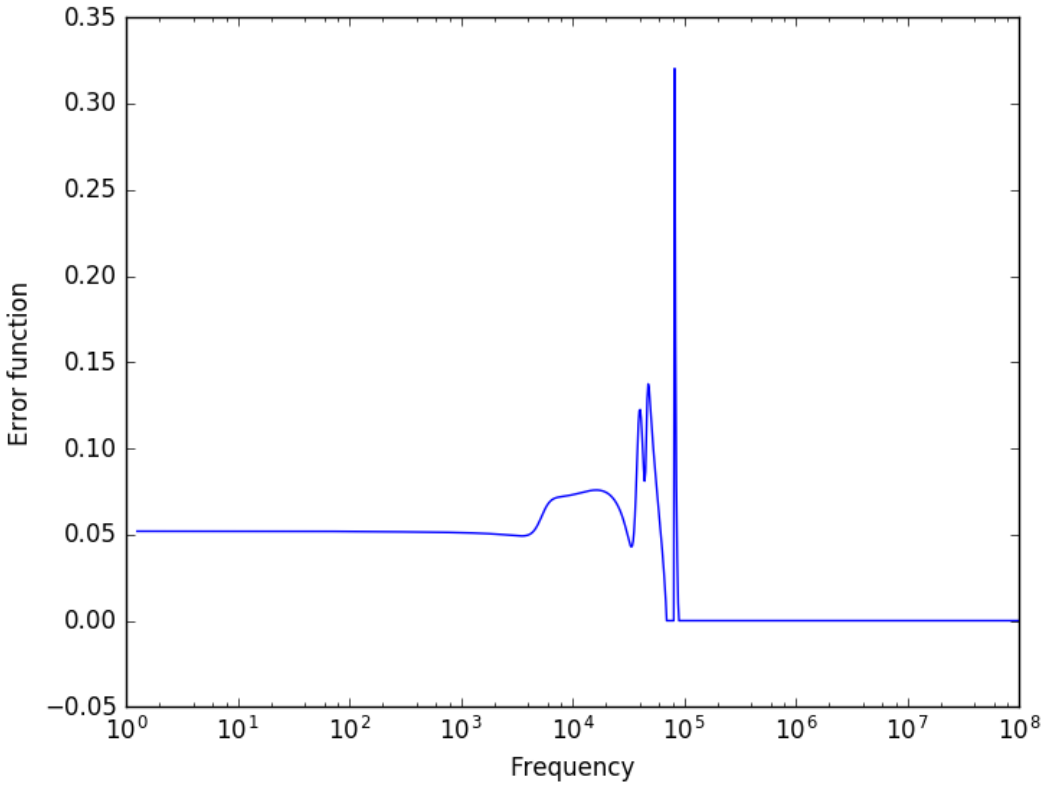

Figure 2.4: Frequency vs Absolute Error plot. (Source: Nuzhat Yamin, Ata Zadehgol, Verification and enforcement of passivity through direct minimal modification of equivalent circuits. Copyright ©2016, IEEE International Symposium on Electromagnetic Compatibility-EMC EUROPE)

$$\sqrt{Z_r^2(\omega) + Z_i^2(\omega)} = \sqrt{(Z_r'(\omega) + R')^2 + (Z_i'(\omega) + R_i')^2} \tag{2.15}$$

where Z_r and Z_i denote real and imaginary parts of impedance before passivity enforcement and Z_r' and Z_i' denote real and imaginary parts of impedance after passivity enforcement.

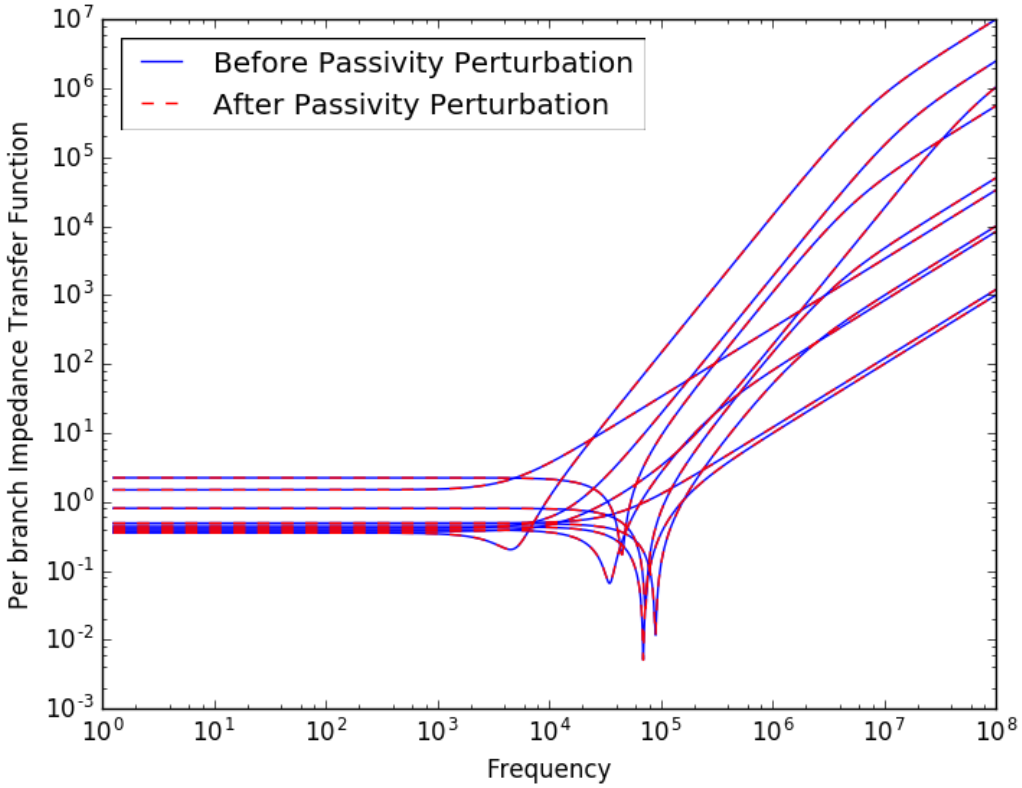

Figure 2.5: Change in Branch Impedance Magnitude response after adding R_i'. (Source: Nuzhat Yamin, Ata Zadehgol, Verification and enforcement of passivity through direct minimal modification of equivalent circuits. Copyright ©2016, IEEE International Symposium on Electromagnetic Compatibility-EMC EUROPE)

2.4 Summary

We presented a new technique for passivity verification and enforcement of single-port network characterized by partial fraction form of transfer function. The new algorithm accurately validates the passivity of a macromodel without needing to construct Hamiltonian

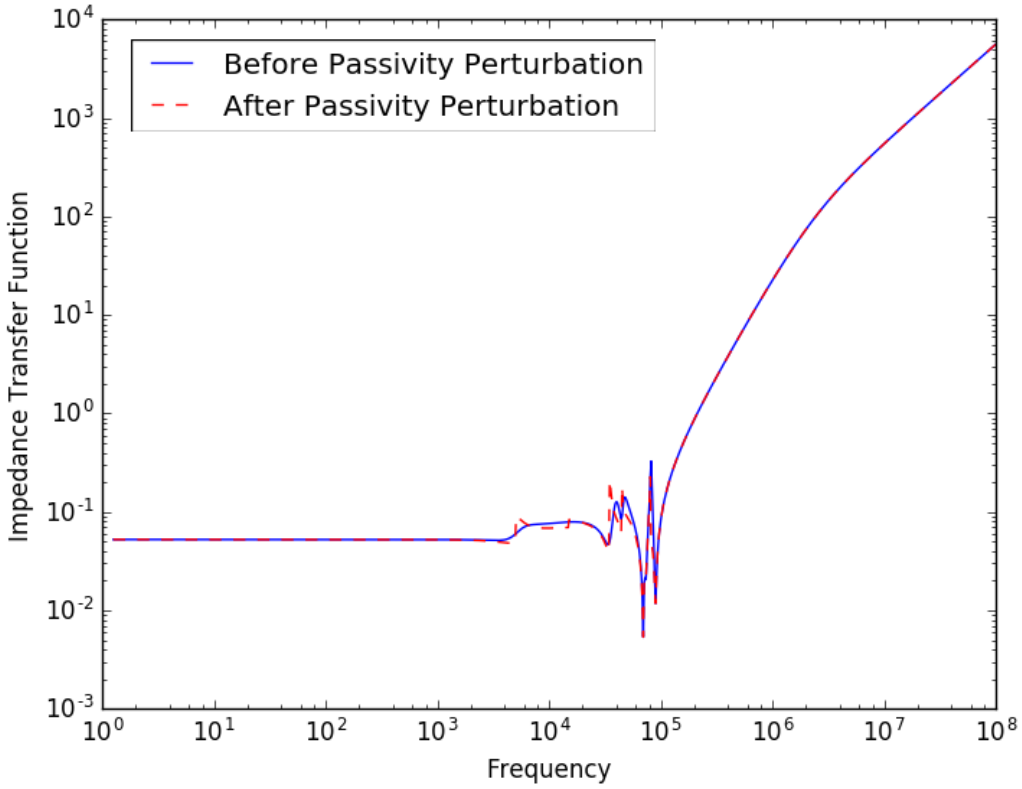

Figure 2.6: Change in Total Impedance Magnitude response after adding R'_i. (Source: Nuzhat Yamin, Ata Zadehgol, Verification and enforcement of passivity through direct minimal modification of equivalent circuits. Copyright ©2016, IEEE International Symposium on Electromagnetic Compatibility-EMC EUROPE)

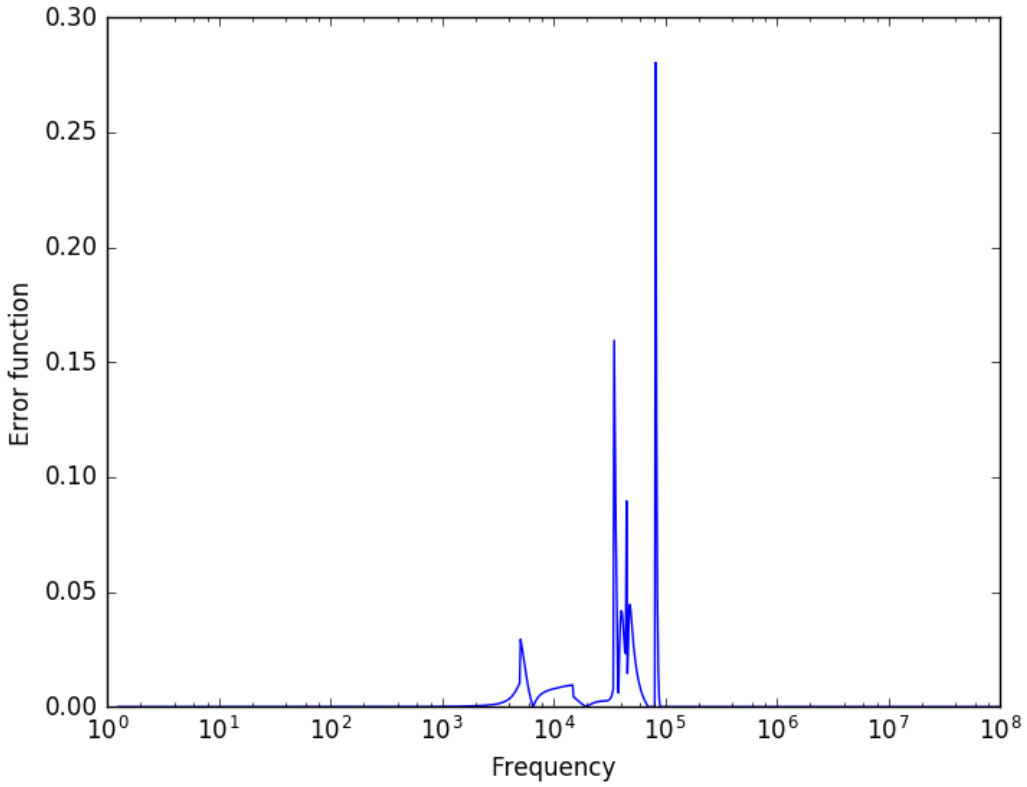

Figure 2.7: Frequency vs Absolute Error plot after adding R_i'. (Source: Nuzhat Yamin, Ata Zadehgol, Verification and enforcement of passivity through direct minimal modification of equivalent circuits. Copyright ©2016, IEEE International Symposium on Electromagnetic Compatibility-EMC EUROPE)

matrix, and overcomes the numerical difficulties associated in determining the imaginary eigenvalues of Hamiltonian matrices. However, the limitation of this method is the associated phase change of the perturbed response. Our future work is to investigate and improve this method to minimize the error related to both phase and magnitude response.

CHAPTER 3

Verification of Passivity by identifying Zero Locations

3.1 Introduction

It is convenient to factor the polynomials in the numerator and denominator, and to write the transfer function in terms of poles and zeros, because the location of the poles and zeros provide qualitative insights into the response characteristics and stability and passivity analysis of a system. An important property of a linear time-invariant passive system, which link the input-output passivity property to frequency-domain conditions, using Parseval's Theorem is given below:

> Given a linear time-invariant system with rational transfer function $h(s)$, i.e. $y(s) = h(s)u(s)$, the system is passive if all the poles of $h(s)$ have real parts less than zero. If the transfer function, $h(s)$ is characterized as impedance transfer function, then the system poles will be defined as the zeros of the admittance transfer function and vice versa. Hence, we develop a method to identify the location of zero in the frequency domain to assess passivity of the system.

In recent years, there has been considerable interest in the study of computing zeros of linear time-invariant systems. Although several algorithms [80], [81] have been proposed in the literature for the computation of the zeros of a linear system, there is still significant potential for improvement. While these methods require formation of large matrices, singular value decomposition and algebraic manipulations, we propose a fairly simpler approach to compute zeros which is a new method to the best of our knowledge. This method has been published in a conference paper entitled "A novel algorithm for computing the zeros of transfer functions by local minima", IEEE Electrical Performance of Electronic Packaging and Systems (EPEPS), San Diego, CA, USA, October 23-26, 2016.

3.2 Computation of zeros of transfer functions by local minima

The algorithm developed in the chapter is derived from the partial fraction form of rational transfer function. The system matrix is formed to get the zeros because the roots of the numerator polynomial is the solution of the determinant of the system matrix. A data set is obtained and plotted to obtain the local minimas which give the location of the zeros of the system. A higher resolution scan is then performed in the vicinity of the local minimas to get the exact zero locations. It is a numerical approach to compute zeros which involve less computation. Primarily, this method is applicable for real zeros only.

The remainder of the section is organized as follows. In Section 3.2.1, we review some useful results regarding definition and properties of zeros of a multi-variable state space system. The algorithm of computing zeros by finding local minima is outlined. Section 3.2.2 and 3.2.3 present numerical results and summary, respectively.

3.2.1 Formulation

The most general state space representation of a linear time-invariant system [82] is,

$$\begin{aligned} \dot{x}(t) &= A \cdot x(t) + B \cdot u(t) \\ y(t) &= C \cdot x(t) + D \cdot u(t) \end{aligned} \tag{3.1}$$

where the system state is $x(t)$, $u(t)$ is the input signal, $y(t)$ is the output signal and A, B, C, D are system state matrices. This system can be represented by its transfer function matrix [82]

$$H(s) = C \cdot (sI - A)^{-1} B + D \tag{3.2}$$

Also, the transfer function is a rational function [83] in the complex variable $s = \sigma + \jmath\omega$, that is

$$H(s) = \frac{N(s)}{D(s)} = \frac{b_m s^m + b_{m-1} s^{m-1} + ... + b_1 s + b_0}{a_n s^n + a_{n-1} s^{n-1} + ... + a_1 s + a_0} \tag{3.3}$$

where σ is the attenuation term in units of (Hz), ω is the angular frequency in units of (rad/s), and imaginary number $\jmath = \sqrt{-1}$. Zeros are defined as the roots of the polynomial of the numerator of a transfer function and poles are defined as the roots of the denominator of a transfer function. For the generalized transfer function [83],

$$H(s) = \frac{N(s)}{D(s)} = \frac{(s - z_1)(s - z_2)\dots(s - z_m)}{(s - p_1)(s - p_2)\dots(s - p_n)} \tag{3.4}$$

where the zeros are $z_1, z_2, \dots z_m$ and poles are $p_1, p_2, ...p_n$.

For real poles and residues, a system transfer function [84] can be characterized by the partial fraction form as follows,

$$H(s) = \sum_{n=1}^{N} \frac{c_n}{s - p_n} \tag{3.5}$$

where c_n is the n^{th} residue, and p_n is the n^{th} pole and N is the total number of poles.

The polynomial $N(s)$ may be obtained by computing the determinant(Det) of the system matrix [85] $\Gamma(s)$.

$$\Gamma(s) = \begin{bmatrix} sI - A & -B \\ C & D \end{bmatrix} \tag{3.6}$$

where $(sI - A) = \begin{bmatrix} s-p_1 & 0 & 0 & 0 \\ 0 & s-p_2 & 0 & 0 \\ & & \ddots & \\ 0 & 0 & & 0 \\ 0 & 0 & 0 & s-p_n \end{bmatrix} : N \times N$, $B = \begin{bmatrix} c_1 \\ c_2 \\ \vdots \\ c_n \end{bmatrix} : N \times 1$, $C = \begin{bmatrix} 1 & 1 & \cdots & 1 \end{bmatrix} : 1 \times N$,

$D = 0$ and I is the identity matrix of size $N \times N$

The determinant of the $\Gamma(s)$ matrix is the characteristic polynomial $N(s)$ in equation (3.3) and (3.4). The zeros of the transfer function $H(s)$ are the roots of the polynomial $N(s)$. In our new technique, we vary σ and get data sets of $(s, \Gamma(s))$. If the condition in

(3.7) holds, then we get a local minima.

$$\Gamma(\Psi_{i-1}) - \Gamma(\Psi_i) > 0 \; and \; \Gamma(\Psi_{i+1}) - \Gamma(\Psi_i) > 0 \tag{3.7}$$

where i is the index number and $\Psi_i = i\Delta\sigma$. The local minimas are the roots of the determinant of $\Gamma(s)$ which imply the zeros of the system.

Algorithm 1: Compute zeros of $H(s)$.

1. Begin with the system transfer function $H(s)$ in the partial fraction form (3.5).
2. Form the block matrix $\Gamma(s)$ as in (3.6) to get the determinant using poles and residues of the transfer function.
3. Compute the determinant of the block matrix for different values of σ ranging from 10% below the value of lowest pole to 10% above the highest pole.
4. Compute the local minimas using condition (3.7) which give the zeros.
5. Increase resolution (samples/decade) in the vicinity of each local minima and get the exact zeros.

3.2.2 Numerical Results

In the following we show an approach for computing zeros, based on the method developed in Section 3.2.1. Let us consider the following transfer function with 10 distinct poles described in [86].

$$\begin{aligned} H(s) = \frac{N(s)}{D(s)} &= \frac{6.29342}{s+541} + \frac{8.97702}{s+7919} + \frac{11.5591}{s+104729} \\ &+ \frac{14.0777}{s+1.29971\times10^{6}} + \frac{16.5554}{s+1.54859\times10^{7}} \\ &+ \frac{19.0053}{s+1.79425\times10^{8}} + \frac{21.4353}{s+2.03807\times10^{9}} \\ &+ \frac{23.8501}{s+2.28018\times10^{10}} + \frac{26.2531}{s+2.52098\times10^{11}} + \frac{3.3673}{s+29} \end{aligned} \tag{3.8}$$

To get the zeros of the transfer function, we vary σ from 10 to 10^{12} by keeping $\omega = 0$. Now, using Algorithm 1, we get 9 local minimas which are shown in Figure 3.1

To obtain the exact value of the zeros, we apply state 5 of Algorithm 1 and increase sample numbers per decade. With increasing number of samples, we get closer to the zeros. The values are given in Tables 3.3 and 3.4

As the number of samples/decade increases, we get closer to the exact zero values given in [86] which are shown in Figure 3.2, 3.3 and 3.4 for $z_2 = -4189.67$

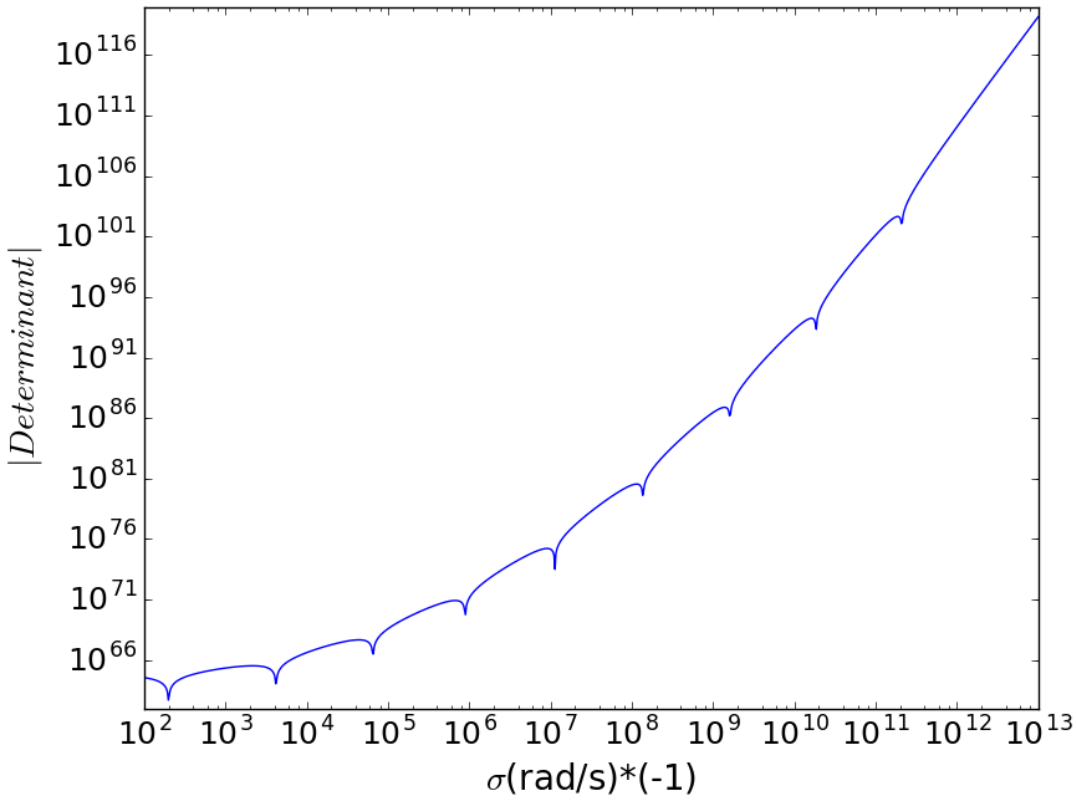

Figure 3.1: σ vs $|Det(\Gamma(x)|)$ Plot. (Source: Nuzhat Yamin, Ata Zadehgol, A novel algorithm for computing the zeros of transfer functions by local minima. Copyright ©2016, IEEE 25th Conference on Electrical Performance Of Electronic Packaging And Systems (EPEPS))

Table 3.1: Value of zeros of equation (3.8) with less number of samples. (Source: Nuzhat Yamin, Ata Zadehgol, A novel algorithm for computing the zeros of transfer functions by local minima. Copyright ©2016, IEEE 25th Conference on Electrical Performance Of Electronic Packaging And Systems (EPEPS))

10 samples/decade	100 samples/decade
-215.443469	-200.92330026
-4641.58883361	-4229.24287439
-59948.42503189	-65793.32246576
-774263.68268113	-890215.08544504
-11672238.64478847	-11233240.32978027
-1.29154967e+08	-1.38488637e+08
-1.66810054e+09	-1.59228279e+09
-1.675788578e+10	-1.83073828e+10
-2.456987705e+11	-2.10490414e+11

Table 3.2: Value of zeros of equation (3.8) with increased number of samples. (Source: Nuzhat Yamin, Ata Zadehgol, A novel algorithm for computing the zeros of transfer functions by local minima. Copyright ©2016, IEEE 25th Conference on Electrical Performance Of Electronic Packaging And Systems (EPEPS))

1000 samples/decade	10000 samples/decade
-199.66424501	-199.72390234
-4193.94395567	-4189.50020707
-65285.21141128	-65250.14155006
-891148.23228402	-891035.46361709
-11299339.38033222	-11308508.80543817
-1.37131472e+08	-1.36997825e+08
-1.60770442e+09	-1.60923942e+09
-1.84614695e+10	-1.83073828e+10
-2.09083769e+11	-2.10490414e+11

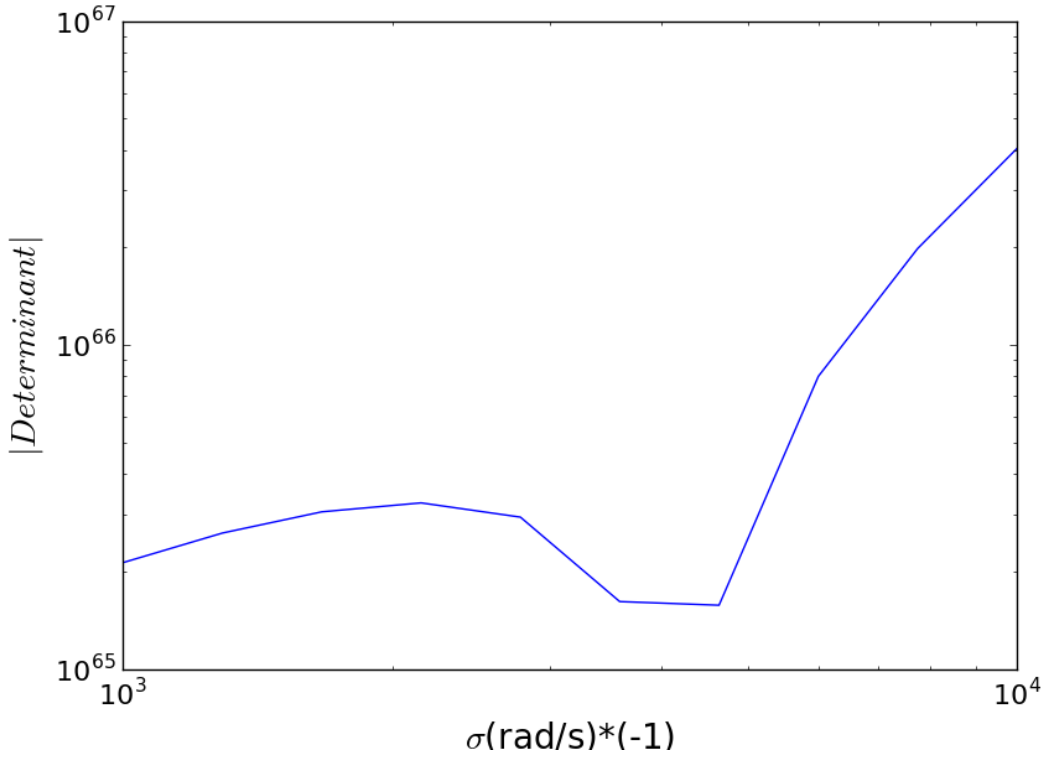

Figure 3.2: Using 10 samples/decade between $\sigma = 10^3 - 10^4$. (Source: Nuzhat Yamin, Ata Zadehgol, A novel algorithm for computing the zeros of transfer functions by local minima. Copyright ©2016, IEEE 25th Conference on Electrical Performance Of Electronic Packaging And Systems (EPEPS))

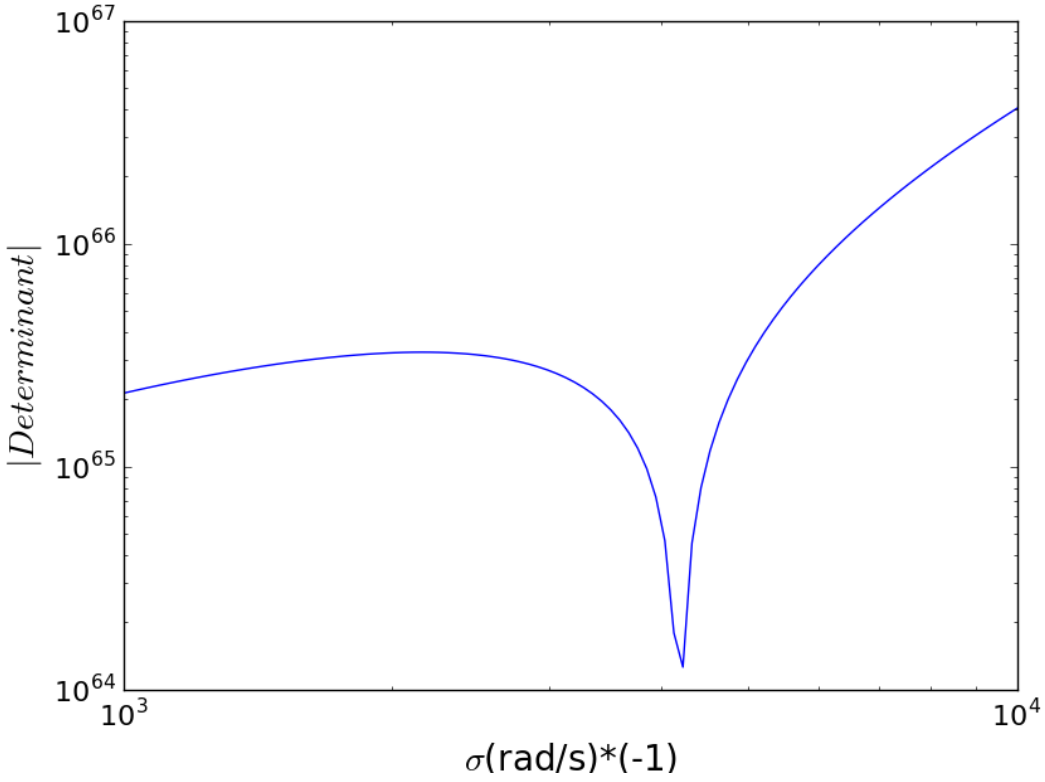

Figure 3.3: Using 100 samples/decade between $\sigma = 10^3 - 10^4$. (Source: Nuzhat Yamin, Ata Zadehgol, A novel algorithm for computing the zeros of transfer functions by local minima. Copyright ©2016, IEEE 25th Conference on Electrical Performance Of Electronic Packaging And Systems (EPEPS))

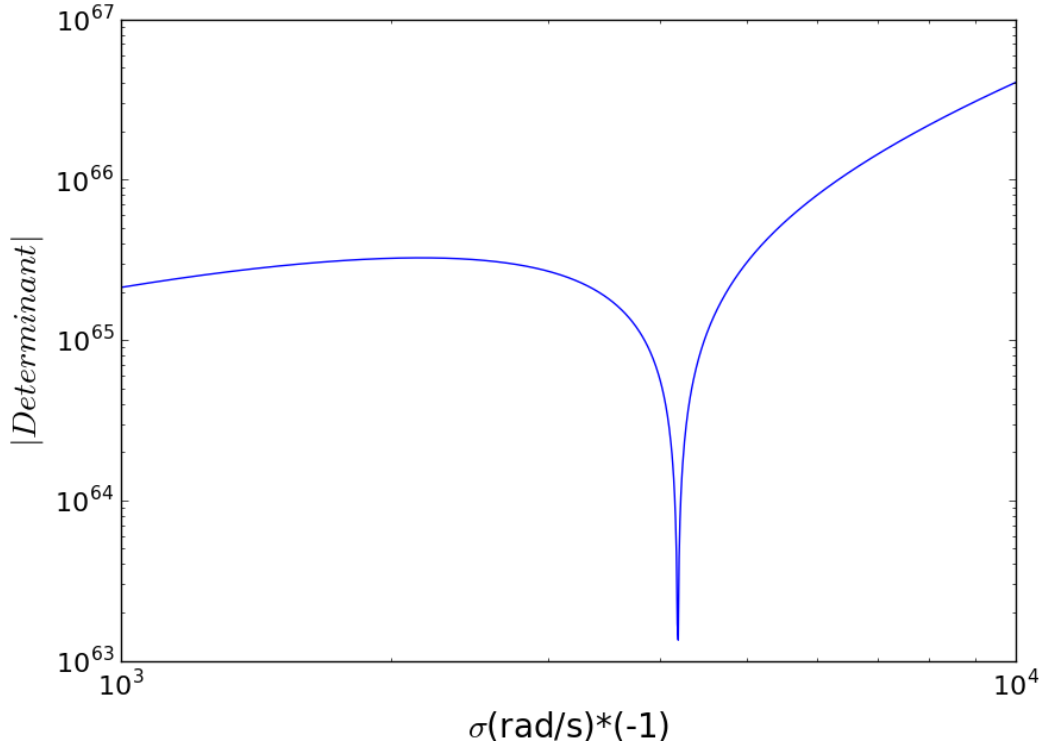

Figure 3.4: Using 1000 samples/decade between $\sigma = 10^3 - 10^4$. (Source: Nuzhat Yamin, Ata Zadehgol, A novel algorithm for computing the zeros of transfer functions by local minima. Copyright ©2016, IEEE 25th Conference on Electrical Performance Of Electronic Packaging And Systems (EPEPS))

3.2.3 Summary

The proposed method can successfully detect all the zeros of a linear time-invariant system realized by rational function in partial fraction form. Numerical examples have been provided to gain insight about the impact of the method computing zeros for system identification and synthesis. This technique can successfully detect zeros of a higher order system with a varying range of zeros. In this section, we use this approach for real poles and zeros. In the following section, we treat the complex conjugate pair of zeros.

3.3 Identifying Complex Zeros by Searching the Laplace-Plane for Local Minima

The algorithm developed in the present section is derived from the work presented in [87] which showed a simpler approach to compute real zeros derived from partial fraction form of rational transfer function. The block matrix is formed and a data set is obtained and plotted to obtain the local minimas which give the location of the zeros of the system. A higher resolution scan is then performed in the vicinity of the local minimas to get the exact zero locations. It is a numerical approach to compute zeros which involve less computation. This method has been published in a conference paper entitled "A Novel Method for Identifying Complex Zeros by Searching the Laplace-Plane for Local Minima", 2017 IEEE International Workshop on Antenna Technology: Small Antennas, Innovative Structures, and Applications, Athens, Greece, March 1-3, 2017.

The remainder of the section is organized as follows. In Section 3.3.1, we review some useful results regarding definition and properties of zeros of a linear-time invariant system. The algorithm of computing zeros by finding local minima is outlined. Section 3.3.2 and 3.3.3 present numerical results and conclusions, respectively.

3.3.1 Formulation

In our proposed technique, we vary σ and ω and get data sets of $(s, \Gamma(s))$. If the condition in (3.9) holds for a point in the complex Laplace s-plane, then it indicates that point is a local minima.

$$\Gamma(\Psi_i, \Omega_j) < \Gamma(\Psi_{i+x}, \Omega_{j+y}) > 0, \tag{3.9}$$

where $(x, y) \in (-1, 0, 1) \quad \text{and} \quad x = y \neq 0 \ \forall \ (x, y)$.

The condition can be elaborated as,

$$\begin{bmatrix} \Psi_{i-1}, \Omega_{j-1} & \Psi_i, \Omega_{j-1} & \Psi_{i+1}, \Omega_{j-1} \\ \Psi_{i-1}, \Omega_j & \Psi_i, \Omega_j & \Psi_{i+1}, \Omega_j \\ \Psi_{i-1}, \Omega_{j+1} & \Psi_i, \Omega_{j+1} & \Psi_{i+1}, \Omega_{j+1} \end{bmatrix} \tag{3.10}$$

where i and j are the index numbers, $\Psi_i = i\Delta\sigma$, $\Theta_j = j\Delta\omega$, $\Delta\sigma$ is the discretization unit along the σ-axis, and $\Delta\omega$ is the discretization unit along the ω-axis. Let us consider a small 3×3 matrix with each sample as the center element. Each sample is checked against the neighbor elements of the matrix. If it is the lowest among all neighboring elements, it is considered to be a local minima.

We are varying σ and ω in the 2^{nd} quadrant (i.e., top left part of the Laplace $\{\sigma, \jmath\omega\}$ plane), as well as along the σ axis (where $\jmath\omega = 0$) because the complex zeros appear in complex-conjugate pairs in the plane, and the real appear on the σ axis. For convenience, it is assumed that the system is stable [77] and we will vary σ at the negative s-plane only as illustrated in Figure 3.5. The local minimas are the roots of the determinant of $\Gamma(s)$ which imply the zeros of the system.

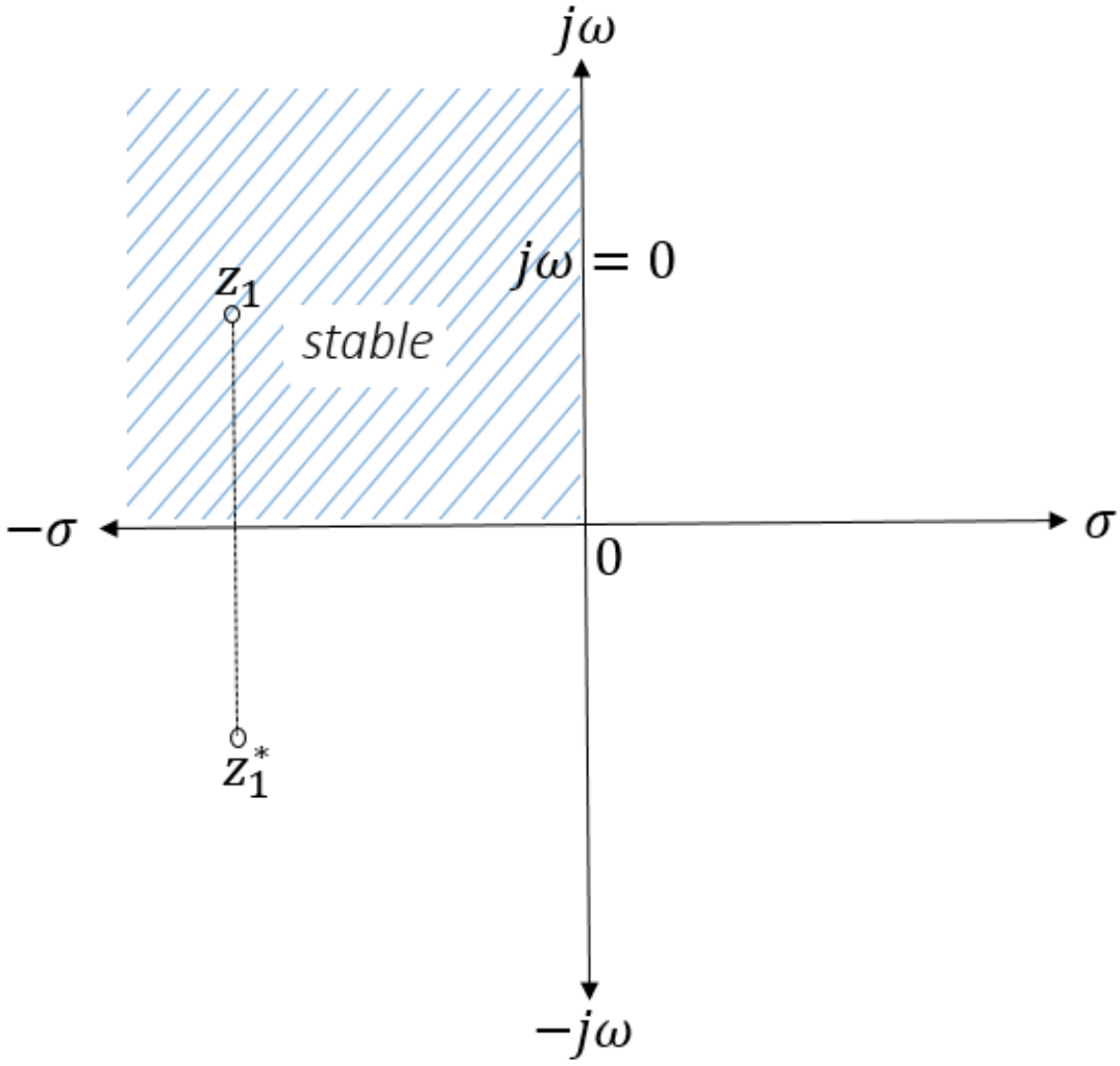

Figure 3.5: Search area in S-plane. (Source: Nuzhat Yamin, Venkatesh Avula, Ata Zadehgol, A Novel Method for Identifying Complex Zeros by Searching the Laplace-Plane for Local Minima. Copyright ©2017, IEEE International Workshop on Antenna Technology (iWAT))

Algorithm 2: Compute zeros of $H(s)$.

1. Begin with the system transfer function $H(s)$ in the partial fraction form (3.5).
2. Form the block matrix $\Gamma(s)$ as in (3.6).
3. Compute the determinant of the block matrix for different values of σ and ω in the second quadrant, ranging from 10% below the value of lowest pole to 10% above the highest pole.
4. Compute the local minimas using condition (3.9) which give the zeros.
5. Increase the resolution (samples/decade) in the vicinity of each local minima to increase precision of the zeros.

3.3.2 Numerical Results

In this section, we verify the proposed algorithm developed in Section 3.3.1 using an example transfer function with 5 complex-conjugate pair of poles/residues.

$$H(s) = \frac{Q(s)}{P(s)} = \frac{c_1}{s-p_1} + \frac{c_1^*}{s-p_1^*} + \frac{c_2}{s-p_2} + \frac{c_2^*}{s-p_2^*} + \frac{c_3}{s-p_3} + \frac{c_3^*}{s-p_3^*} + \frac{c_4}{s-p_4} + \frac{c_4^*}{s-p_4^*} + \frac{c_5}{s-p_5} + \frac{c_5^*}{s-p_5^*}, \tag{3.11}$$

where it is,

$$c_1 = -3.2246 \times 10^{-10} - 1.9637 \times 10^{-10}\jmath,$$

$$c_2 = 1.2282 \times 10^{-5} + 1.09675 \times 10^{-5}\jmath,$$

$$c_3 = 1.802 \times 10^{-6} - 4.3369 \times 10^{-6}\jmath,$$

$$c_4 = 0.0041 - 0.0004\jmath,$$

$$c_5 = 0.4959 + 0.02735\jmath$$

$$p_1 = -59 + 130\jmath,$$

$$p_2 = -630 + 5140\jmath,$$

$$p_3 = -1500 + 2100\jmath,$$

$$p_4 = -7.5 \times 10^4 - 9.3 \times 10^5\jmath,$$

$$p_5 = -5.9 \times 10^6 + 8.1 \times 10^7\jmath$$

The zeros are independently found as follows,

$$z_{1,2} = -75.1193 \pm 112.7468\jmath$$

$$z_{3,4} = -255.9859 \pm 522.1755\jmath$$

$$z_{5,6} = -5642.9085 \pm 53636.3132\jmath$$

$$z_{7,8} = -823818.7331 \pm 7273165.113\jmath$$

$$z_9 = -62.425$$

To verify the proposed method of computing zeros, we vary σ and ω from -10^8 to -10. Now, using Algorithm 2, we get 5 local minimas which are shown in Figure 3.6. Since, the complex zeros appear in complex-conjugate pairs, it suffices to search for only one-half of the complex-conjugate pair in the 2^{nd} quadrant (i.e., the top left part of the Laplace s-plane in Figure 3.5, where $\sigma \leq 0 \wedge \omega > 0$) by varying ω from 10 to 10^8; thus search in the 3^{rd} quadrant (i.e., bottom left s-plane where $\sigma < 0 \wedge \omega < 0$) can be skipped! Also, we assume system is stable; thus, we skip search in the 1^{st} quadrant (top right) and the 4^{th} quadrant (bottom right), where $\sigma > 0$.

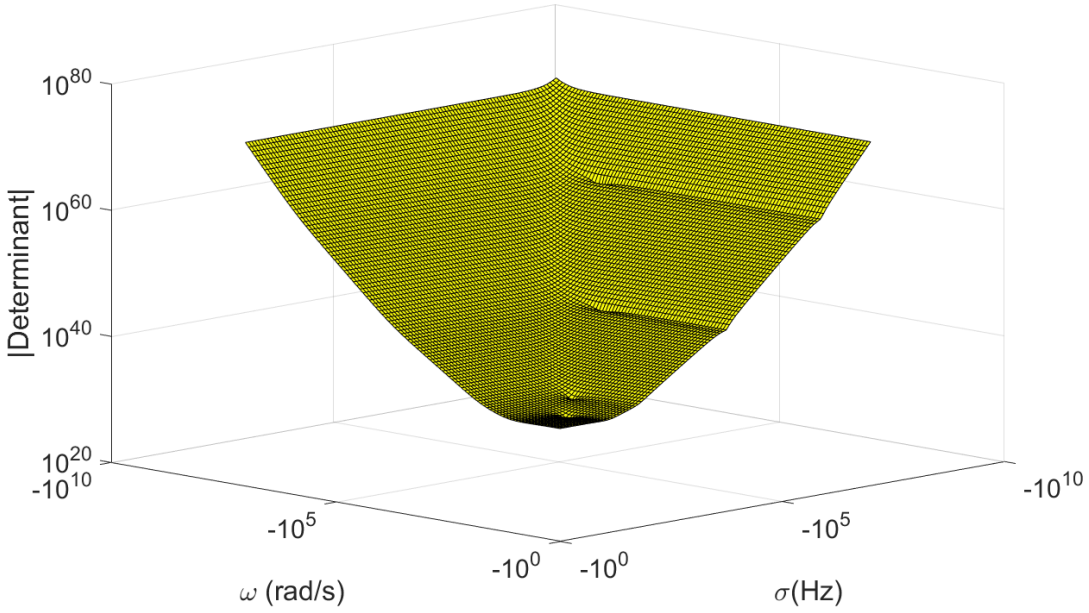

Figure 3.6: The 3-dimensional surface plot of $|Det(\Gamma(s)|)$ vs. $\{\sigma, \omega\}$. (Source: Nuzhat Yamin, Venkatesh Avula, Ata Zadehgol, A Novel Method for Identifying Complex Zeros by Searching the Laplace-Plane for Local Minima. Copyright ©2017, IEEE International Workshop on Antenna Technology (iWAT))

To increase precision of the zero locations, we apply step 5 of Algorithm 2 and increase sample numbers per decade. With increasing number of samples, we calculate zeros with higher accuracy. The values are given in Table 3.3 and Table 3.4.

As the number of samples/decade increases, we get closer to the exact zero values which are shown in Figures 3.7 and 3.8. We get two zeros in the region between $\sigma = -10^3$ to -10.

Table 3.3: Value of zeros of equation (3.11) with less number of samples. (Source: Nuzhat Yamin, Venkatesh Avula, Ata Zadehgol, A Novel Method for Identifying Complex Zeros by Searching the Laplace-Plane for Local Minima. Copyright ©2017, IEEE International Workshop on Antenna Technology (iWAT))

10 samples/decade	50 samples/decade
-61.111	-62.245
$-64.5775 - 107.7217\jmath$	$-76.3209 - 111.1498\jmath$
$-258.3099 - 556.5119\jmath$	$-252.9710 - 511.9096\jmath$
$-5301.4593 - 49537.3736\jmath$	$-5302.8455 - 50594.2087\jmath$
$-858685.9374 - 7113734.3\jmath$	$-858685.9287 - 7115438.8\jmath$

Table 3.4: Value of zeros of equation (3.11) with increased number of samples. (Source: Nuzhat Yamin, Venkatesh Avula, Ata Zadehgol, A Novel Method for Identifying Complex Zeros by Searching the Laplace-Plane for Local Minima. Copyright ©2017, IEEE International Workshop on Antenna Technology (iWAT))

100 samples/decade	500 samples/decade
-62.626	-62.245
$-74.2484 - 112.8509\jmath$	$-74.0135 - 112.1169\jmath$
$-252.3714 - 519.0048\jmath$	$-255.4127 - 522.2322\jmath$
$-5669.8967 - 52877.6459\jmath$	$-5654.0623 - 53990.8932\jmath$
$-839343.012195 - 7300177.4\jmath$	$-824453.86279 - 7346257.6\jmath$

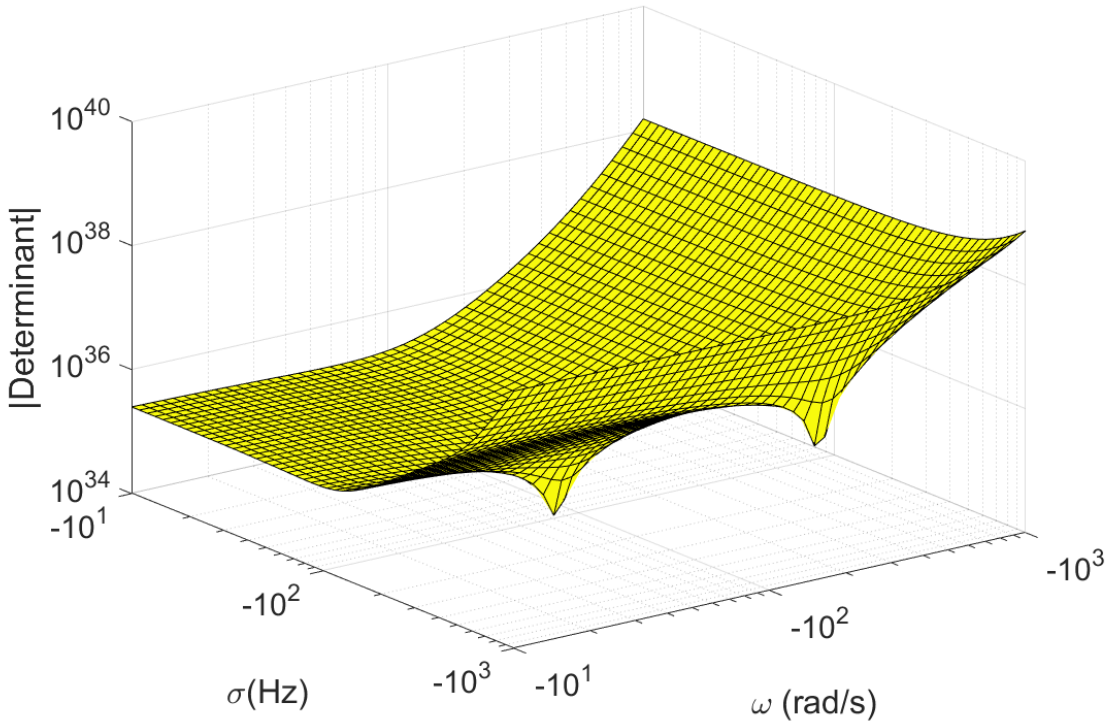

Figure 3.7: Plot of $|Det(\Gamma(s)|)$ vs. $\{\sigma, \omega\}$ using 50 samples/decade, zoomed-in to vicinity of two local minima points. (Source: Nuzhat Yamin, Venkatesh Avula, Ata Zadehgol, A Novel Method for Identifying Complex Zeros by Searching the Laplace-Plane for Local Minima. Copyright ©2017, IEEE International Workshop on Antenna Technology (iWAT))

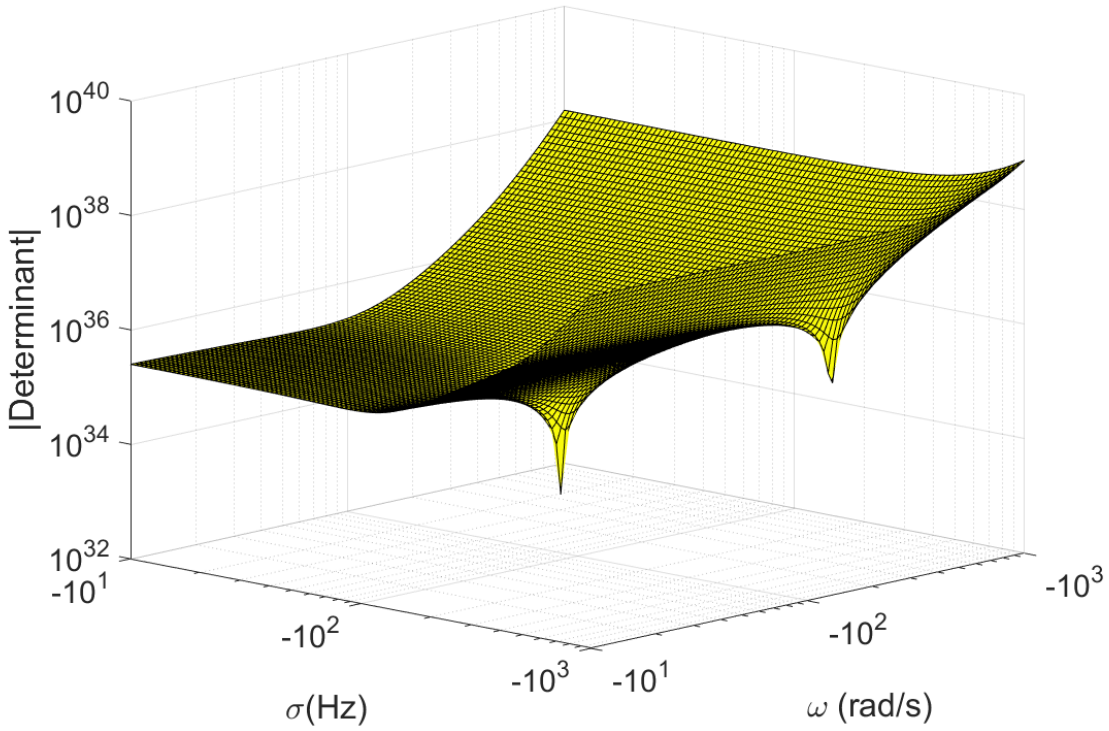

Figure 3.8: Plot of $|Det(\Gamma(s)|)$ vs. $\{\sigma, \omega\}$ using 100 samples/decade, zoomed-in to vicinity of two local minima points. (Source: Nuzhat Yamin, Venkatesh Avula, Ata Zadehgol, A Novel Method for Identifying Complex Zeros by Searching the Laplace-Plane for Local Minima. Copyright ©2017, IEEE International Workshop on Antenna Technology (iWAT))

This method can be applied to any antenna to extract the zeros from the antenna response. We have demonstrated the algorithm to find the zeros from the poles and residues of a coax patch antenna. We conducted the local minima search in the range from -10^2 to -10^7 and obtained two local minimas shown in Figure 3.9.

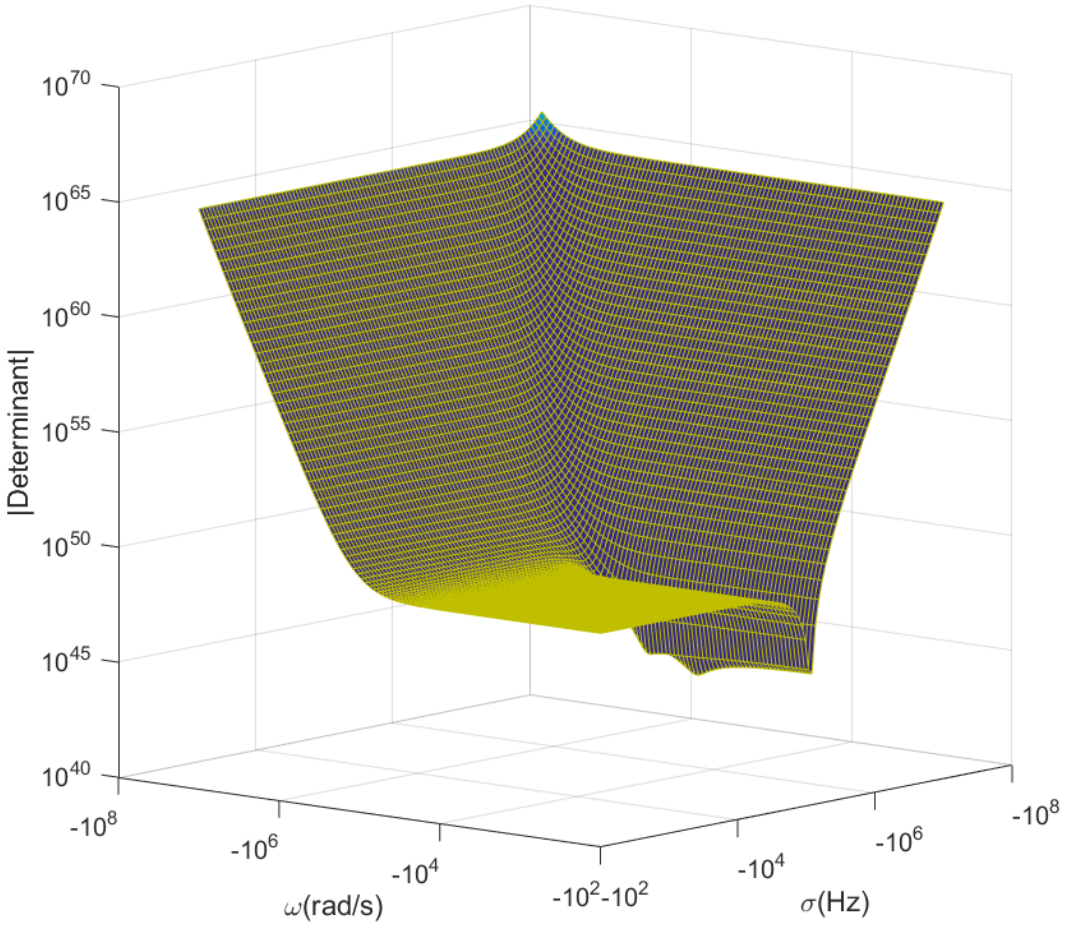

Figure 3.9: The 3-dimensional surface plot of $|Det(\Gamma(s)|)$ vs. $\{\sigma, \omega\}$. (Source: Nuzhat Yamin, Venkatesh Avula, Ata Zadehgol, A Novel Method for Identifying Complex Zeros by Searching the Laplace-Plane for Local Minima. Copyright ©2017, IEEE International Workshop on Antenna Technology (iWAT))

Now, as we perform the search with higher resolution (300 samples/decade) and closed region ($\sigma = -10^5$ to $-10^3, \omega = -10^6$ to -10^4), we get 4 local minimas resulting in zeros at $z_1 = -1473.45 - 111196.77j$, $z_2 = -2684.46 - 119717.13j$, $z_3 = -3883.09 - 115378.32j$ and $z_4 = -10046.25 - 109163.17j$ as shown in Figure 3.10.

However, the limitation associated with this method is that it would not work properly on a noisy response. This algorithm may detect the noisy dips as zeros. In the next section, this issue will be addressed.

3.3.3 Summary

A method is proposed to identify the complex zeros of a rational transfer function in partial fraction form, by searching the 2-dimensional Laplace s-plane for local minima of magnitude of a block matrix. The method is successfully applied to a numerical example with five pairs of complex-conjugate poles/residues.

3.4 Computing the Zeros of Noisy Transfer Functions by Local Minima

The algorithm developed in the present section is derived from the partial fraction form of rational transfer function. The system matrix is formed to get the zeros because the roots of the numerator polynomial is the solution of the determinant of the system matrix. This work is an improvement on the previous technique of computing zeros based on local minima [87] which gives the location of the zeros of the system. If the signal suffers from noise, the previous technique will detect numerous local minimas and will fail to distinguish between noise and actual zeros. Therefore, we present a new method to overcome this problem to compute the zeros successfully from noise affected data. It is a numerical approach to compute zeros which involve less computation. Primarily, this method is applicable for real zeros only.

The remainder of the section is organized as follows. In Section 3.4.1, we review some useful results regarding definition and properties of zeros of a linear, time-invariant state space system. The algorithm of computing zeros from noise affected data is outlined. Section 3.4.2 and 3.4.3 present numerical results and summary, respectively.

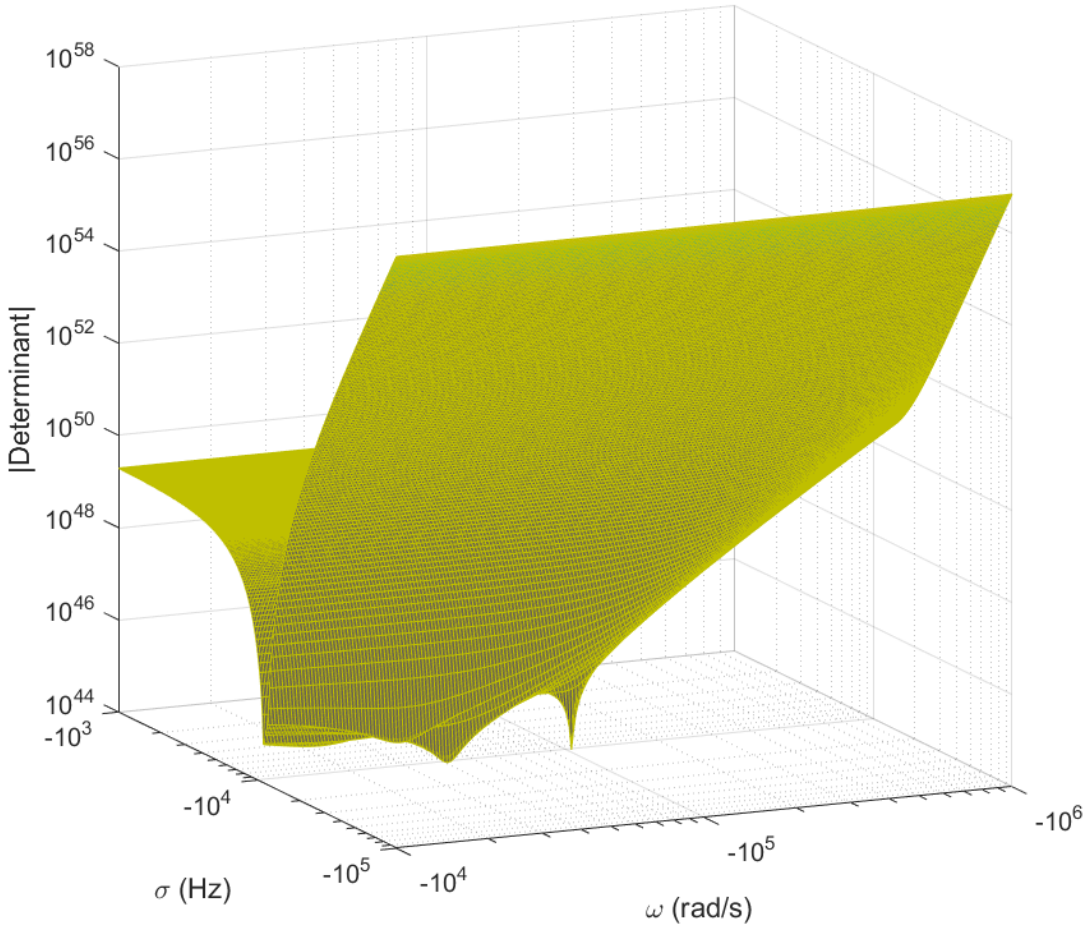

Figure 3.10: The 3-dimensional surface plot of $|Det(\Gamma(s)|)$ vs. $\{\sigma, \omega\}$. using 300 samples. (Source: Nuzhat Yamin, Venkatesh Avula, Ata Zadehgol, A Novel Method for Identifying Complex Zeros by Searching the Laplace-Plane for Local Minima. Copyright ©2017, IEEE International Workshop on Antenna Technology (iWAT))

3.4.1 Formulation

In this method, we vary σ and get data sets of $(s, \Gamma(s))$. If the condition in (3.12) holds, then we get a local minima [87]

$$\Gamma(\Psi_{i-1}) - \Gamma(\Psi_i) > 0 \; and \; \Gamma(\Psi_{i+1}) - \Gamma(\Psi_i) > 0 \tag{3.12}$$

where i is the index number and $\Psi_i = i\Delta\sigma$. The local minimas are the roots of the determinant of $\Gamma(s)$ which imply the zeros of the system.

When the signal is affected by noise, condition (3.12) detects numerous local minimas which fail to detect the actual zeros. A threshold has been defined as such, the actual zeros can be distinguished from numerous local minimas. If the following condition holds given that (3.12) holds, then we get the actual zeros.

$$(\Gamma(\Psi_{i-1}) \div \Gamma(\Psi_i))^2 + (\Gamma(\Psi_{i+1}) \div \Gamma(\Psi_i))^2 > Th \tag{3.13}$$

where Th is the threshold. From our simulation, we have observed that when $Th = 8$, the algorithm detects zeros correctly when minimum $SNR = 8$ (refer to equations (3.13) and (3.15)). If we keep increasing the threshold level, we observe that the technique fails to detect actual zeros at higher threshold values, because higher threshold value ignores the typical ratio value of the actual zeros. Numerical examples have been demonstrated to show the relation of threshold to SNR and number of erroneous zeros.

Algorithm 3: Compute zeros of $H(s)$.

1. Begin with the system transfer function with Noise $H(s)$ in the partial fraction form (3.5).
2. Using poles and residues of the transfer function, form the block matrix $\Gamma(s)$ as in (3.6).
3. Compute the determinant of the block matrix for different values of σ ranging from 10% below the value of lowest pole to 10% above the highest pole.
4. Compute the local minimas using condition (3.12).
5. Check forward and backward ratio using condition (3.13) to distinguish actual zeros from all the local minimas due to noise.

3.4.2 Numerical Results

In the following we show an approach for computing zeros from noise affected data, based on the method developed in section 3.4.1. Let us consider the following transfer function with 11 distinct poles described in [86].

$$\begin{aligned} H(s) = \frac{N(s)}{D(s)} = &\frac{0.03136}{s+341} + \frac{0.06512}{s+8929} + \frac{0.10146}{s+103839} \\ &+ \frac{0.12824}{s+1.37471\times10^{6}} + \frac{0.11185}{s+1.47359\times10^{7}} \\ &+ \frac{-0.0176}{s+1.40325\times10^{8}} + \frac{0.13749}{s+2.48407\times10^{9}} \\ &+ \frac{0.13094}{s+2.38418\times10^{10}} + \frac{0.13069}{s+2.49498\times10^{11}} \\ &+ \frac{0.0333}{s+2.78732\times10^{12}} + \frac{0.1471}{s+32} \end{aligned} \tag{3.14}$$

To get the zeros of the transfer function, we vary σ from 10 to 10^{13} by keeping $\omega = 0$. Now, using 1-4 of Algorithm 3, we get 10 local minimas which are shown in Figure 3.11

We get the following values of zeros. Since it is a known system, the zeros match with the obtained values.

$$z_1 = -284.0884, \;\; z_2 = -6468.6077$$

$$z_3 = -73767.9760, \;\; z_4 = -993109.1814$$

$$z_5 = -11969557.0236, \;\; z_6 = -144264395.122$$

$$z_7 = -1996642450.11, \;\; z_8 = -20384933982.5$$

$$z_9 = -213958887134.0, \;\; z_{10} = -2.72543253128\times10^{12}$$

Now, we apply two different random noise on the signal with a normal distribution to measure the effectiveness of the technique with increased SNR.

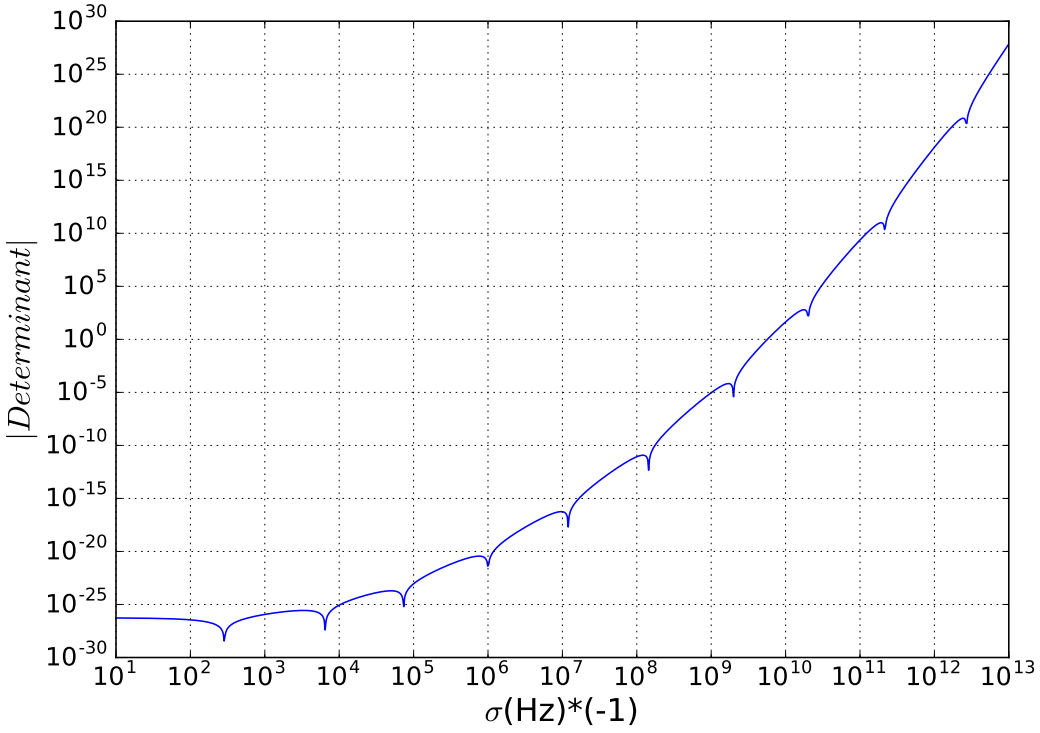

Figure 3.11: σ vs $|Det(\Gamma(x)|$ Plot

Case I: Additive Noise

The average of the noise is 0 and standard deviation is 3. When we apply 4 of Algorithm 3, it detects numerous local minimas which make it impossible to detect the actual zeros as shown in Figure 3.12.

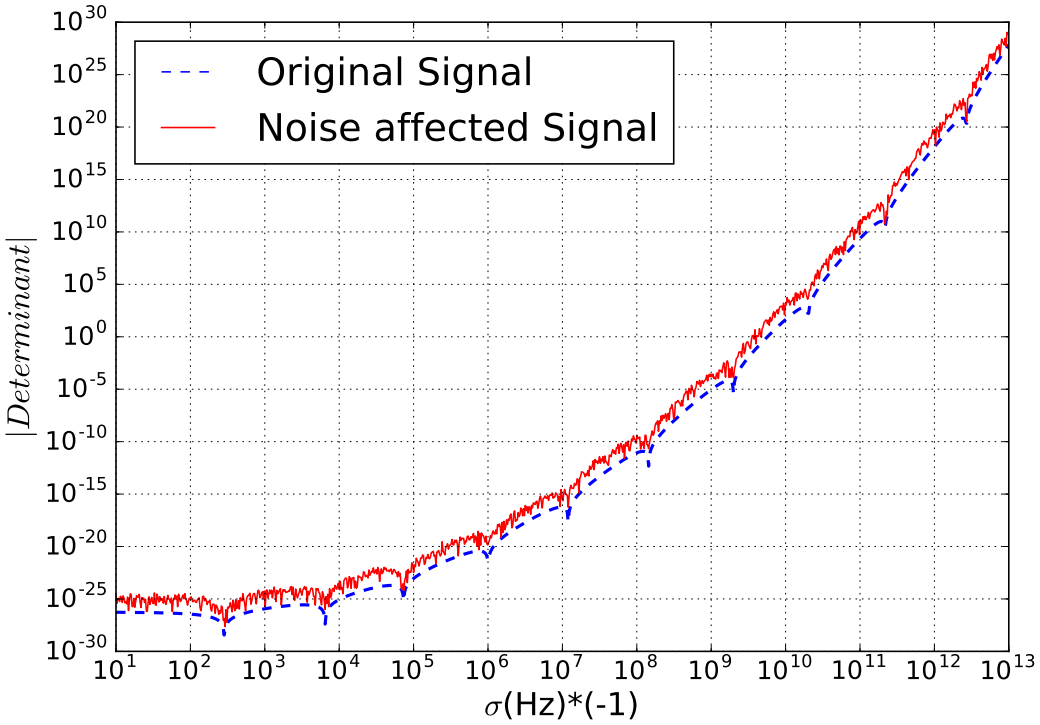

Figure 3.12: σ vs $|Det(\Gamma(x)|$ Plot

As we apply the condition stated in (3.13), it detects the zeros correctly. We vary the noise level from .05 to 10 to check the effectiveness of the technique. The technique works fine upto Noise level $0.125 \times Signal$ and it starts to generate erroneous zeros as the Signal to Noise ratio (SNR) goes down. We have varied threshold starting from $Th = 4$ to $Th = 8$ to show the minimum SNR required for the technique to detect zeros correctly as shown in Figure 3.13.

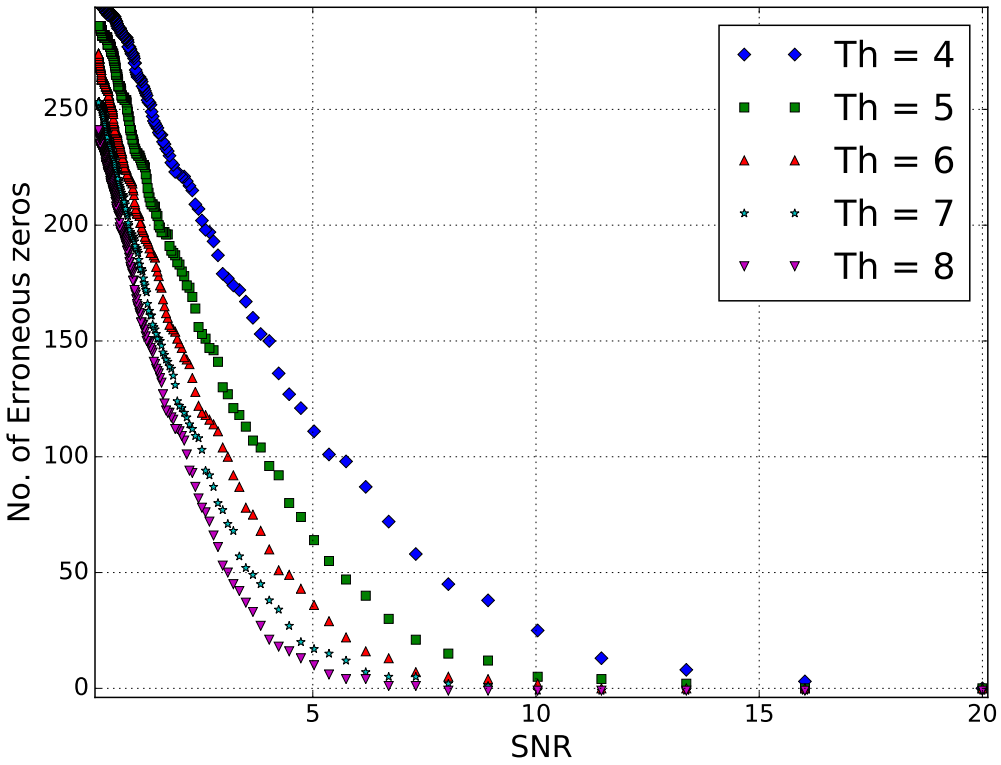

Figure 3.13: SNR vs No. of Erroneous Zeros Plot (Case -I)

Case II: Additive and Subtractive Noise

In this case, we have taken a random noise (Figure 3.14) with average 0 and standard deviation 0.4. The noise level has been varied from $-1.01 \times Signal$ to $+1.01 \times Signal$. From Figure 3.15, we can see that as SNR approaches zero (the noise level approaches infinity), the number of erroneous zeros goes up at different threshold values.

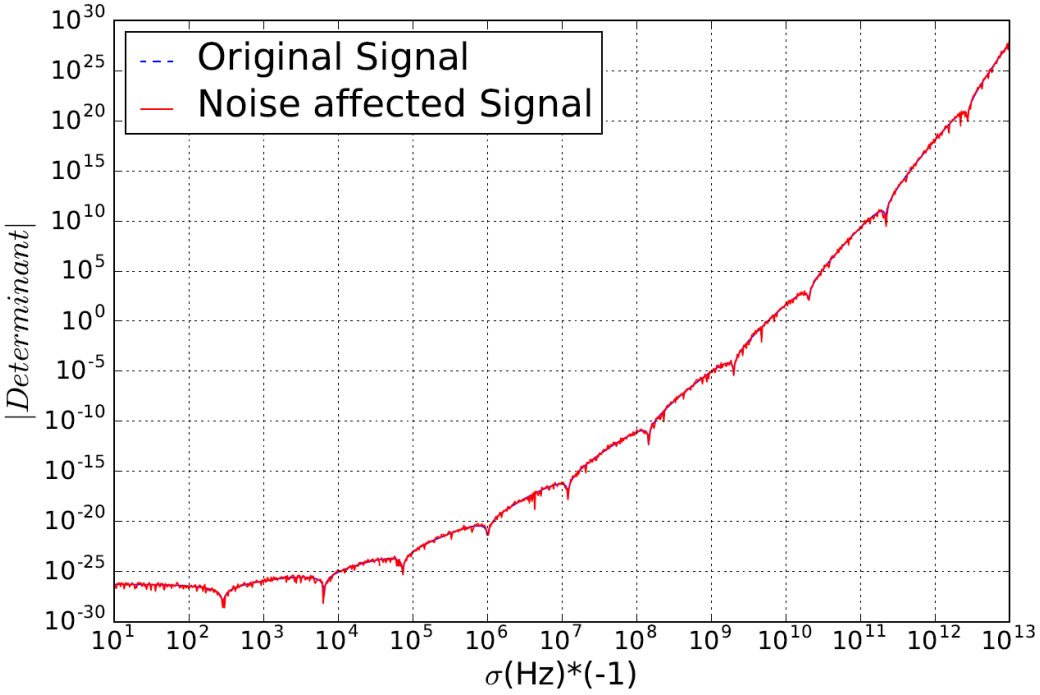

Figure 3.14: σ vs $|Det(\Gamma(x)|$ Plot

We have normalized our signal with the following normalization factor, so that they could be compared relevantly.

$$\log_{10}(N.F) = \frac{\log_{10}(min) + \log_{10}(max)}{2} \tag{3.15}$$

where N.F is the normalization factor.

It has been observed that our technique can detect zeros upto a certain amount of noise

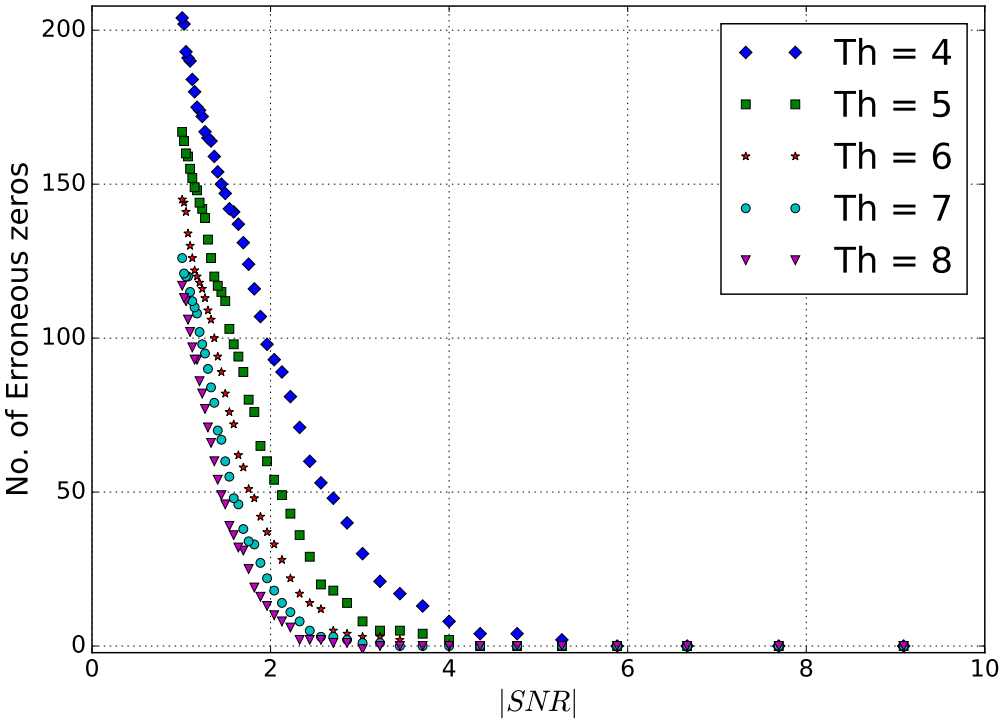

Figure 3.15: SNR vs No. of Erroneous Zeros Plot (Case-II)

level. As the noise level goes high, the signal loses its significance and it becomes difficult to detect the actual zeros.

3.4.3 Summary

In this section, we propose an improved zero computing method for noise affected data. This method successfully detects the zeros of a linear, time-invariant system realized by rational function considering the effect of unwanted noise. First, the technique computes the local minimas of the signal. In the second step, we use a threshold to distinguish the actual zeros from numerous local minimas for computation of zeros from noise affected data. Numerical examples have been provided to gain insight about the impact of the method computing zeros for system identification and synthesis.

3.5 Conclusion

As passivity can be assessed by looking at the zero locations in the frequency domain according to Parseval's Theroem, we developed three methods to detect the zeros of rational transfer fuction from local minima. At first, the algorithm has been developed for real values of zeros only. Then, the algorithm has been improved into detect the complex zeros also. Lastly, the algorithm has been developed so that it can extract the zeros from a noisy transfer function. However, the last method can only detect the real zeros from noise which can be further extended to build up to detect complex zeros as well from noisy transfer function.

CHAPTER 4

Method for DC-Extrapolation of the Frequency-Domain Responses using Three Sample Points

4.1 Introduction

Modern high speed digital interconnect systems have reached multi-gigahertz data rates and there is constant demand for even higher speed. Compared to RF signals which are narrowband signals, digital signals have wide bandwidth from DC to about the third harmonic frequency [88]. Therefore, while RF systems do not need to consider low frequencies, digital systems must consider the very low frequency behavior. Inaccurate modeling of the low frequency region can produce erroneous results in digital system simulations. Interconnect models are usually extracted using Vector Network Analyzer (VNA) or field solvers in the frequency domain. However, it is difficult to accurately capture the low frequency response using the frequency domain methods and full-wave Maxwell's equation solvers have difficulties in solving the low-frequency response [89].

The S-parameters in low frequency are still significant for system characterization. Although it is possible to extract the low frequency response using VNAs of different bandwidth, or using a time-domain reflectometry (TDR) [88], it is preferable to obtain data towards DC from known information by extrapolation. Simple extrapolation approaches like zero-padding or two-point linear are used in some simulators. A more elaborate approach may use a rational polynomial to curve-fit the tabulated data [4], which implicitly extrapolates the data beyond the original range.

In this chapter, we use a novel iterative method for finding an equivalent set of poles and residues of a system from its discrete frequency domain response to obtain the low frequency response, that are typically not available by conventional measurements. In Section 4.2 we present the formulation and algorithm of our method, followed by numerical examples and

discussion in Section 4.3 and 4.4. We summarize in Section 4.5.

4.2 Formulation

Let us assume a given frequency domain transfer function $H_g(\omega)$ that consists of N samples, $H_g(\omega) = \{[\omega_1, h_1], [\omega_2; h_2], \cdots, [\omega_N, h_N]\}$ defined over discrete frequency samples $\omega = \{\omega_1, \omega 2, \cdots, \omega_N\}$. The frequency domain model of a system contains its responses at discrete frequencies over a predefined bandwidth. According to the method described in reference [90], which is called PRESS (Pole Residue Equivalent System Solver), combination of individual local transfer functions matching at multiple local subsets can be effective in approximating the given model's frequency response. PRESS uses the given frequency response and equates with the error that is minimized repeatedly by performing local fits at the subset which are centered at peak position of error magnitude. After fitting one particular subset, the remaining error response is defined as the fitted response, from which another subset is taken for local fitting. Until the approximate global fit is achieved within a predefined accuracy, the local fitting is performed iteratively. By discarding the unstable local fit poles at each local fit stage, stability is enforced. The peaks of error are also traversed until a stable pole is found [28].

As mentioned before, PRESS uses a subset Ψ for each iteration, which is centered at position of peak of magnitude of error. It is defined as a collection of selected consecutive points from the sampled transfer function. For our thesis, we use a three point subset: $\Psi = \{[\omega_L, h_L], [\omega_C, h_C], [\omega_R, h_R]\}$ where ω_L, ω_C and ω_R are the left, center and right samples, respectively. The center sample is fixed at the lowest transition point of the transfer function to extrapolate to DC point in low frequency region. We use the following fit equation that consists of a pair of complex conjugate poles and residues:

$$H_{approx}(s) = \frac{c}{s-p} + \frac{c^*}{s-p^*} + \frac{s-p_1}{c_1} \tag{4.1}$$

where $c, p \in Complexes$ and $c_1,\ p_1 \in Reals$. For the three point subset, using (4.1) we have:

$$H_{approx}(\jmath\omega_L) = h_L; \quad H_{approx}(\jmath\omega_C) = h_C;$$
$$H_{approx}(\jmath\omega_R) = h_R$$

By expanding these equations and equating the real and imaginary part as given in reference [90], the six unknowns c_r, c_i, p_r, p_i, c_1 and p_1 can be solved numerically, where $c = c_r + \jmath c_i$ and $p = p_r + \jmath p_i$.

The detailed algorithm for obtaining the values of the unknowns is described in reference [90]. The key point here is selecting the subset samples. We have chosen the center sample frequency at the critical point (minima or maxima) at the lowest available frequency sample of the macromodel. The left and right samples are chosen at close proximity of the center sample frequency.

The method is summarized in Algorithm 4 below.

Algorithm 4: Algorithm for DC extrapolation of frequency response

Input : H is the known frequency response.
Output: H_{est} is the approximated frequency response.
1 **if** *Local maxima or minima found at* $\omega = \omega_i$ **then**
2 | Set $\omega_i = \omega_C$
3 **end**
4 Set ω_L and ω_R to the left and right of center sample, respectively at close proximity.
5 Use equation 4.1 to extrapolate frequency response to DC point using ω_L, ω_C and ω_R.

4.3 Numerical Example

In order to validate our extrapolation algorithm, numerical example of a finite frequency response is presented in this section. In this example, we consider a finite frequency response of a transfer function which is given as follows,

$$H(s) = \frac{N(s)}{D(s)} = \sum_{n=1}^{6} \frac{c_n}{s - p_n} + \frac{c_n^*}{s - p_n^*} + \frac{s - p_7}{c_7}$$

where,

$$c_1 = -64.2857,\ c_2 = -142.86 + 71.43\jmath,$$

$$c_3 = -171.43 + 2142.86\jmath,\ c_4 = -4285.714 + 50000\jmath,$$

$$c_5 = -1428.57 + 104285.71\jmath,\ c_6 = -2857.14 + 128571.43\jmath,$$

$$c_7 = 7.1428 \times 10^5,\ p_1 = -42.8571,\ p_2 = -7.1429 + 100\jmath,$$

$$p_3 = -28.5714 + 2571.4286\jmath,\ p_4 = 8.571 \times 10^3 + 6.42 \times 10^4\jmath,$$

$$p_5 = -3.2857 \times 10^4 + 1.14 \times 10^5\jmath,$$

$$p_6 = -1.428 \times 10^3 + 6.4285 \times 10^4\jmath,\ p_7 = -1.4285 \times 10^4$$

The lowest transition point is obtained at frequency $77.228\,rad/s$, so it is chosen as the center frequency, ω_c. The other two sample frequencies are chosen as $\omega_L = 73.745\,rad/s$ and $\omega_r = 97.269\,rad/s$. Using step 5 of Algorithm 4, H_{approx} is obtained as follows :

$$H_{approx}(s) = \frac{-146.214 - 54.941\jmath}{s - (-7.385 - 99.492\jmath)} + \frac{-146.214 + 54.941\jmath}{s - (-7.385 + 99.492\jmath)} + \frac{s - 659.812}{79.349}$$

where,

$$c_r = -146.214,\ c_i = -54.941\jmath,$$

$$p_r = -7.385,\ p_i = -99.492\jmath,$$

$$c_1 = 79.349,\ p_1 = 659.812$$

The fitted transfer function and the original transfer function are depicted in Figure 4.1. From Figure 4.1, we can find that the extrapolation results agree very well with the original transfer function for a finite frequency response. So, for insufficient data samples at very low frequency region, our method can extrapolate very well to DC point.

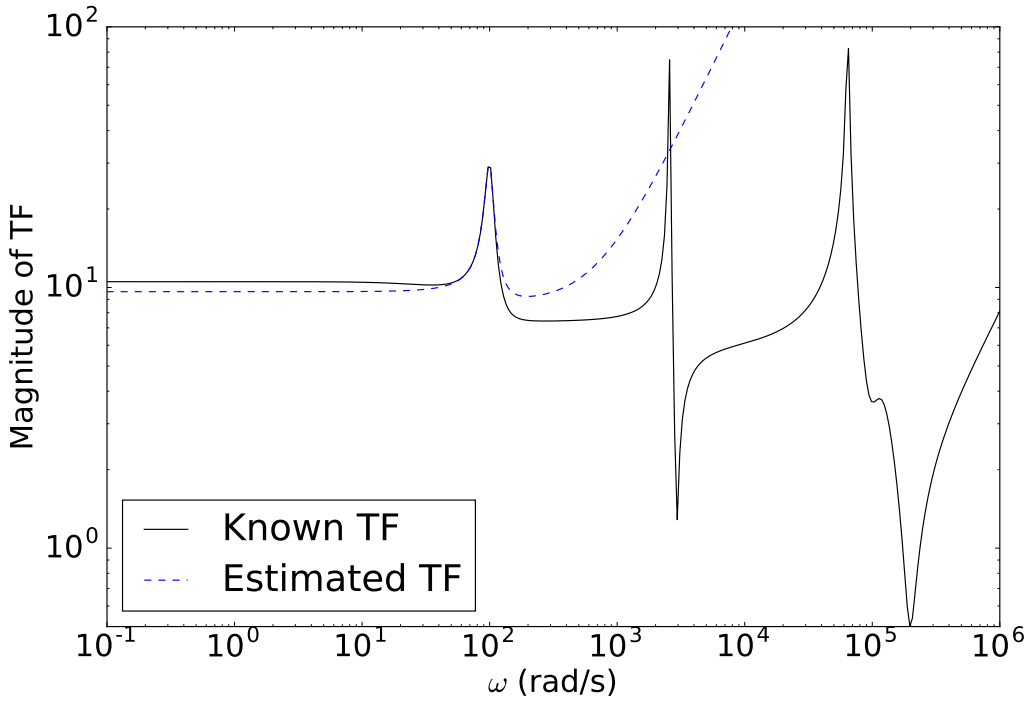

Figure 4.1: Comparison of transfer functions of a finite frequency response. The figure shows a good match at low frequency region.

4.4 Discussion

A numerical example is presented here to demonstrate the efficiency of our method. For convenience, it is assumed that our given frequency response is passive and stable. Our estimated frequency response obtained by extrapolation can be verified for passivity and stability by the cellular approach described in [77]. The pole/residue form of the fitted transfer function (4.1) can be transformed to equivalent circuit branch as shown in Figure 4.2.

In the circuit, R_a, L, R_b and C_1 are given by equation (18) of [77] and $C_2 = \frac{1}{c_1}$ and $G = \frac{-p_1}{c_1}$.

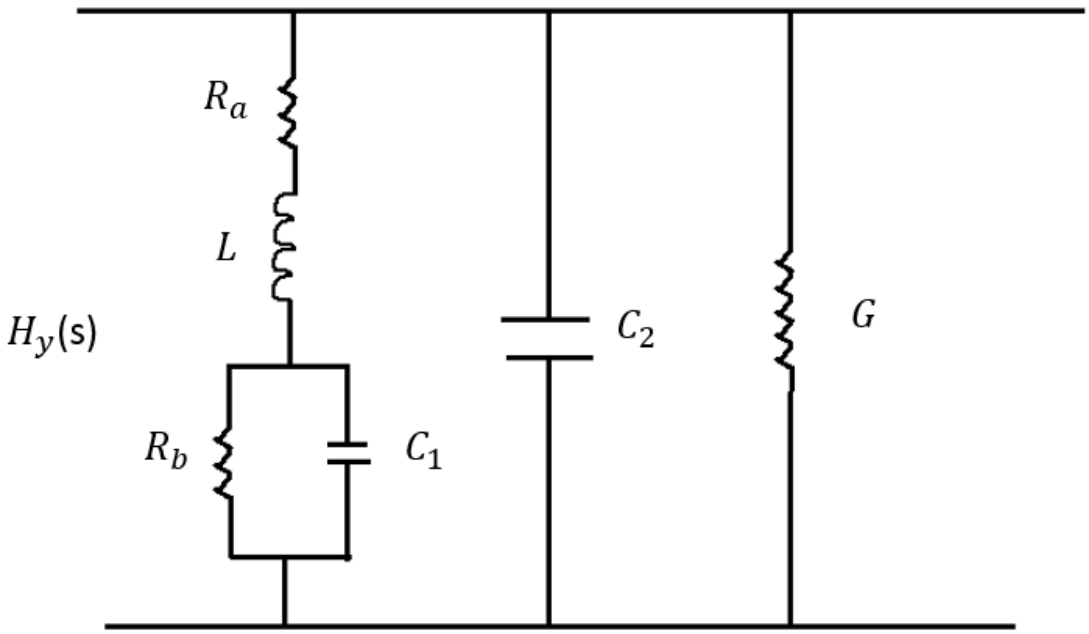

Figure 4.2: Equivalent Circuit form of the fitted frequency response

Here,

$$\begin{aligned} Z_1(\omega) &= R_a + \jmath\omega L + (\frac{1}{R_b} + \jmath\omega C_1)^{-1} \\ Z_2(\omega) &= \frac{1}{\jmath\omega C_2} \\ Z_3(\omega) &= \frac{1}{G} \end{aligned} \tag{4.2}$$

The individual RLRC branches corresponding to each partial fraction term are connected in parallel and the total impedance of the whole system for each frequency is given by:

$$Z_T(\omega) = \frac{1}{\sum_{m=1}^{M} \frac{1}{Z(\omega_m)}}, \tag{4.3}$$

where M is the maximum number of frequency samples and m denotes the number of branches.

So, using the technique described in Chapter 2, the estimated response can be varified for passivity. If $Z_T(\omega) > 0$, $H_{approx}(s)$ is also passive. Also, passivity can be enforced using

direct minimal modification of equivalent circuit method described in Chapter 2.

For the numerical example used here, we get two poles, $-7.385 - 99.492\jmath$ and $-7.385 + 99.492\jmath$ for H_{approx}. Since, the poles are in the left half plane, it is evident that our approximated frequency response is stable. For passivity verification, we apply the technique used in [91] and we get the eqivalent circuit of figure 4.2 where $R_a = 0.1026\ \Omega$, $R_b = -0.8628\ \Omega$, $L = -0.0034\ H$, $C_1 = -0.02589\ F$, $C_2 = 0.0126\ F$ *and* $G = -8.3153\ S$. C_2 is an ideal capacitor and it does not have any effect on the passivity of the system. The total impedance is found to be less than zero for this case which implies that the approximated response is non-passive. We apply the direct minimal modification passivity enforcement technique [91] to the response and the magnitude of the total impedance of the approximated response (before and after enforcement) has been plotted for comparison in Figure 4.3.

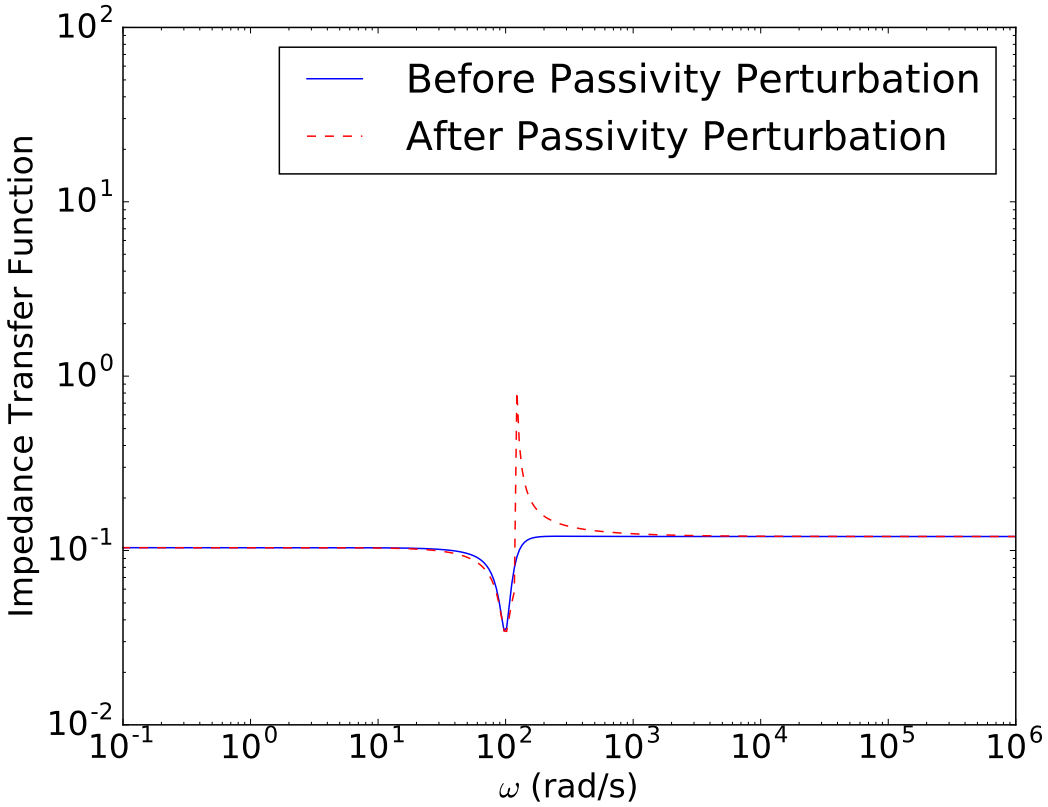

Figure 4.3: Magniture of total impedance of H_{approx} before and after enforcement

From Figure 4.1, it is evident that our region of interest is below $\omega = 77.228\, rad/s$ and in Figure 4.3, we can see that transfer function is minimally changed below $\omega = 77.228\, rad/s$. So, passivity is enforced without affecting our approximated response at the region of interest.

4.5 Summary

In this chapter, we develop a technique to extrapolate frequency domain response of macro-models to DC-point using 3-point data samples. This is a simple method of estimating frequency response beneath the lowest available frequency sample of the model. It has been verified that the estimation is passive and stable. This method would not work for insufficient data sample around the lowest transition point of the transfer function. However, accurate estimate of the transfer function has been demonstrated in different cases where sufficient data were available.

CHAPTER 5

Passive Model Order Reduction

Model-order reduction (MOR) is a widely used technique to reduce the order of the extracted interconnect circuits for fast circuit simulation. For years, researchers have been studying numerical methods to preserve the essential structures of the reduced order system. Special attention has been paid to maintain the passivity of the reduced-order model. In this thesis, we focus on a projection based Model Order Reduction technique called the Second Order Arnoldi Method for Passive Order Reduction [76]. This method is a modified version of the Rayleigh–Ritz orthogonal projection based Second Order Arnoldi Reduction method [92].

5.1 Formulation

To work with this method, we first obtain poles and residues of the large order system extracted from the S-parameter data using PRESS algorithm [90]. These poles and residues are then transformed into equivalent circuit elements using the cellular approach [77]. Modified Nodal Analysis is then performed on the equivalent circuit branch to obtain the full order C, G, Γ, E and B matrices where these are matrices of capacitance, conductance, inductance and incidence matrices for inductance and current sources respectively. For our circuit topology of n branches in Figure 5.1 the MNA formulation can be applied if a current source J is connected to the circuit in parallel. For 2 branches, the MNA formulation is as follows:

$$V_1(G_{a_1} + G_{a_2}) - V_{2_1}G_{a_1} - V_{2_2}G_{a_2} = J \tag{5.1}$$

$$-V_1G_{a_1} + V_{2_1}G_{a_1} + i_1 = 0; -V_1G_{a_2} + V_{2_2}G_{a_2} + i_2 = 0 \tag{5.2}$$

$$C_1\frac{dV_{3_1}}{dt} + V_{3_1}G_{b_1} - i_1 = 0; C_2\frac{dV_{3_2}}{dt} + V_{3_2}G_{b_2} - i_2 = 0 \tag{5.3}$$

$$L_1\frac{di_1}{dt} - V_{2_1} + V_{3_1} = 0; L_2\frac{di_2}{dt} - V_{2_2} + V_{3_2} = 0 \tag{5.4}$$

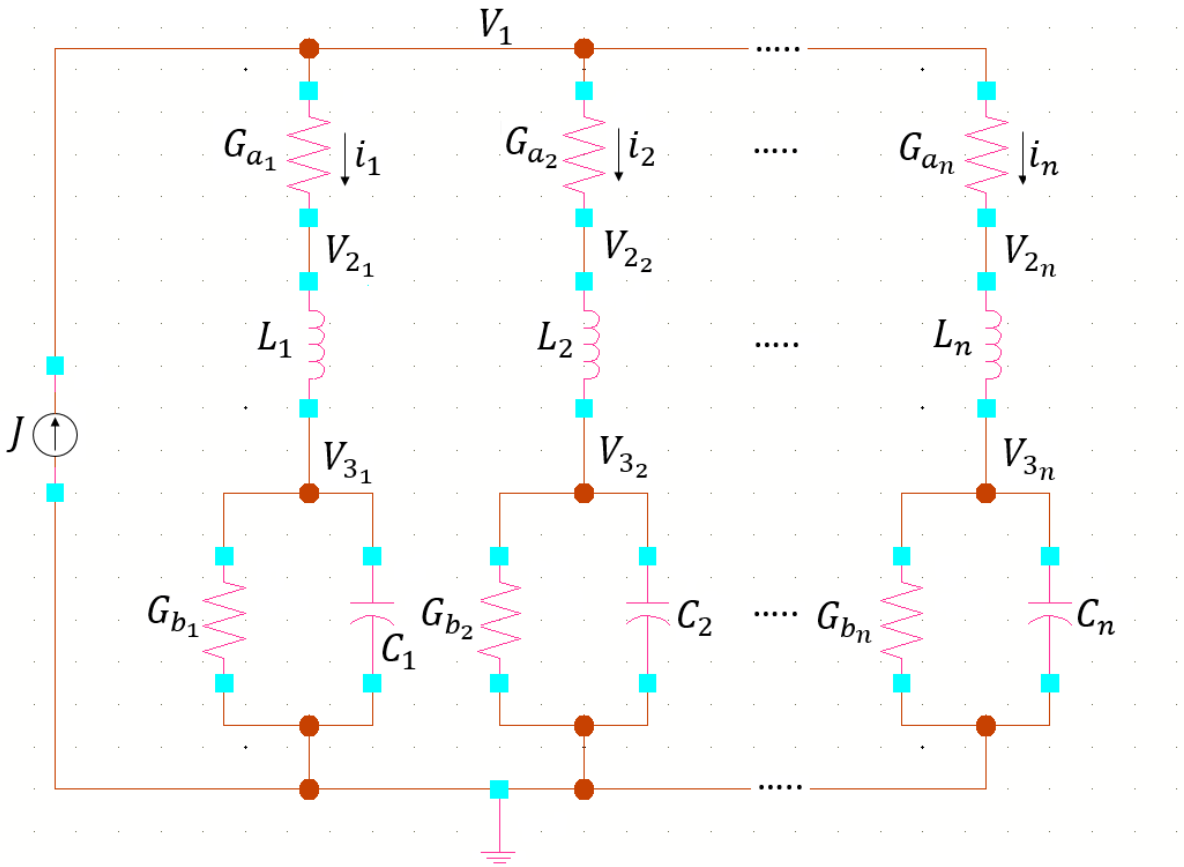

Figure 5.1: Example of circuit topology used to apply MNA formulation

From these formulations, we form $C : N \times N$, $G : N \times N$, $\Gamma : N \times N$ and $B : N \times 1$ matrices according to following pattern where $N = 2n + 1$ and n is the number of branches and $\Gamma = EL^{-1}E^T$

$$C = \begin{bmatrix} 0 & 0 & 0 & \dots & 0 \\ 0 & 0 & 0 & \dots & 0 \\ 0 & 0 & C_1 & \dots & 0 \\ \vdots & \vdots & \vdots & \ddots & \vdots \\ 0 & 0 & 0 & \dots & C_N \end{bmatrix} ; \; G = \begin{bmatrix} G_{a_1} + G_{a_2} & -G_{a_1} & 0 & \dots & 0 \\ -G_{a_1} & G_{a_1} & 0 & \dots & 0 \\ 0 & 0 & G_{b_1} & \dots & 0 \\ \vdots & \vdots & \vdots & \ddots & \vdots \\ 0 & 0 & 0 & \dots & G_{b_N} \end{bmatrix} \tag{5.5}$$

$$L = \begin{bmatrix} L_1 & 0 & 0 \\ \vdots & \ddots & \vdots \\ 0 & 0 & L_n \end{bmatrix} ; \; B = \begin{bmatrix} 1 \\ 0 \\ \vdots \end{bmatrix} \tag{5.6}$$

Now, we apply SAPOR [92] algorithm on these input matrices and obtain projection matrix Q. By performing projection operation using $C_r = Q^T C Q, G_r = Q^T G Q, \Gamma_r = Q^T \Gamma Q$, and $B_r = Q^T B$, we get the reduced order matrices where C_r, G_r, Γ_r and B_r are reduced order capacitance, conductance, inductance and incident current matrices respectively. This orthogonal projection ensures positive semi-definiteness of the matrices leading to ensure passivity of the system.

5.2 Numerical Results

We have demonstrated this Passive Model Order Reduction Method on varying orders of systems to obtain reduced order models. In the following figures, we show a reduction progression of a (41×41) order system getting reduced to (30×30) and preserving the response almost accurately.

At first, we have extracted 40 complex conjugate pairs of poles and residues of the system

using PRESS algorithm, which then transformed into 20 sets of R_a, L, R_b and C elements using equations 2.5 of cellular approach. Then using MNA formulations, we have formed C, G and Γ matrices of order 41×41. On these matrices, SAPOR [76] algorithm has been applied and an orthonormal Q matrix has been generated as the output. By performing orthonormal projection on the original matrices, we have reduced the system order to (30×30) completely preserving the response.

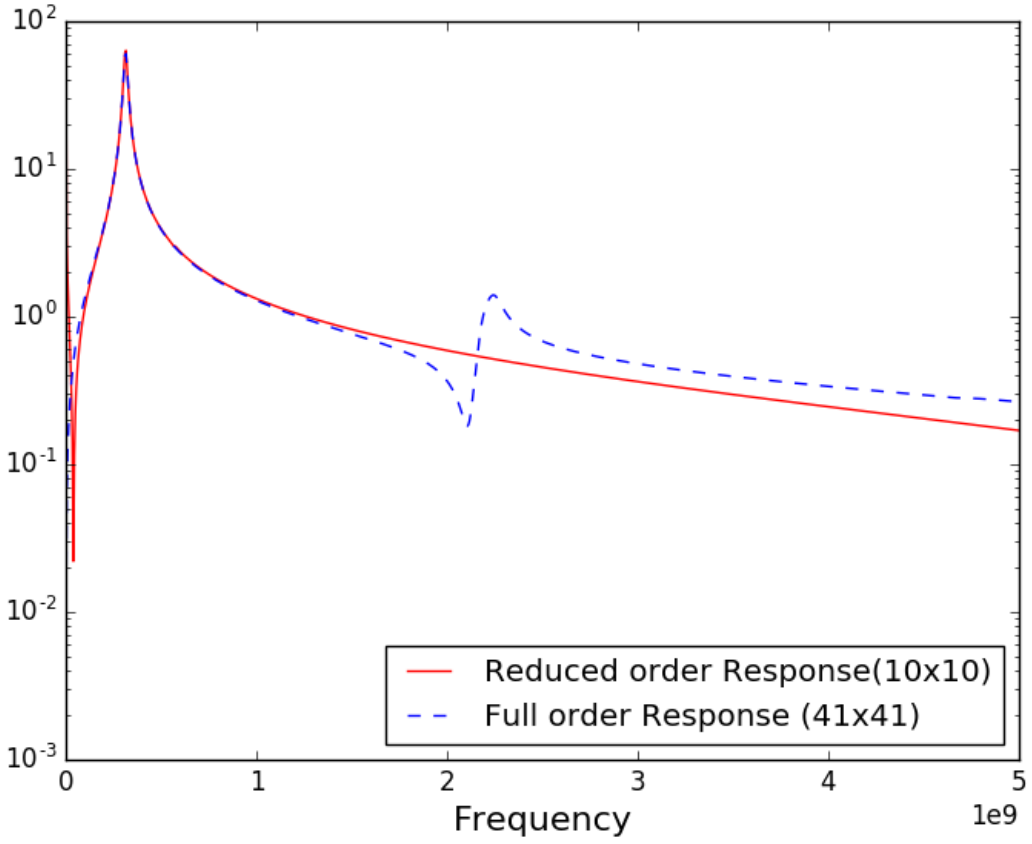

Figure 5.2: The large order system (41x41) reduced to (10x10) system

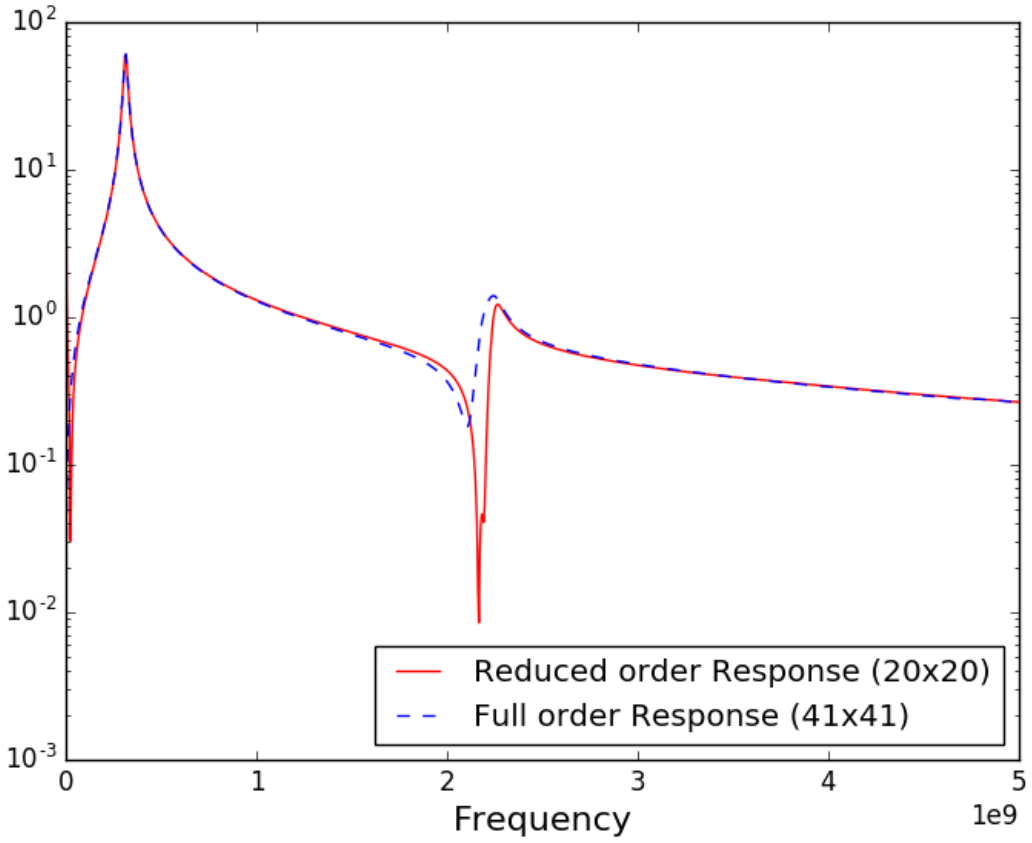

Figure 5.3: The large order system (41x41) reduced to (20x20) system with almost matched response

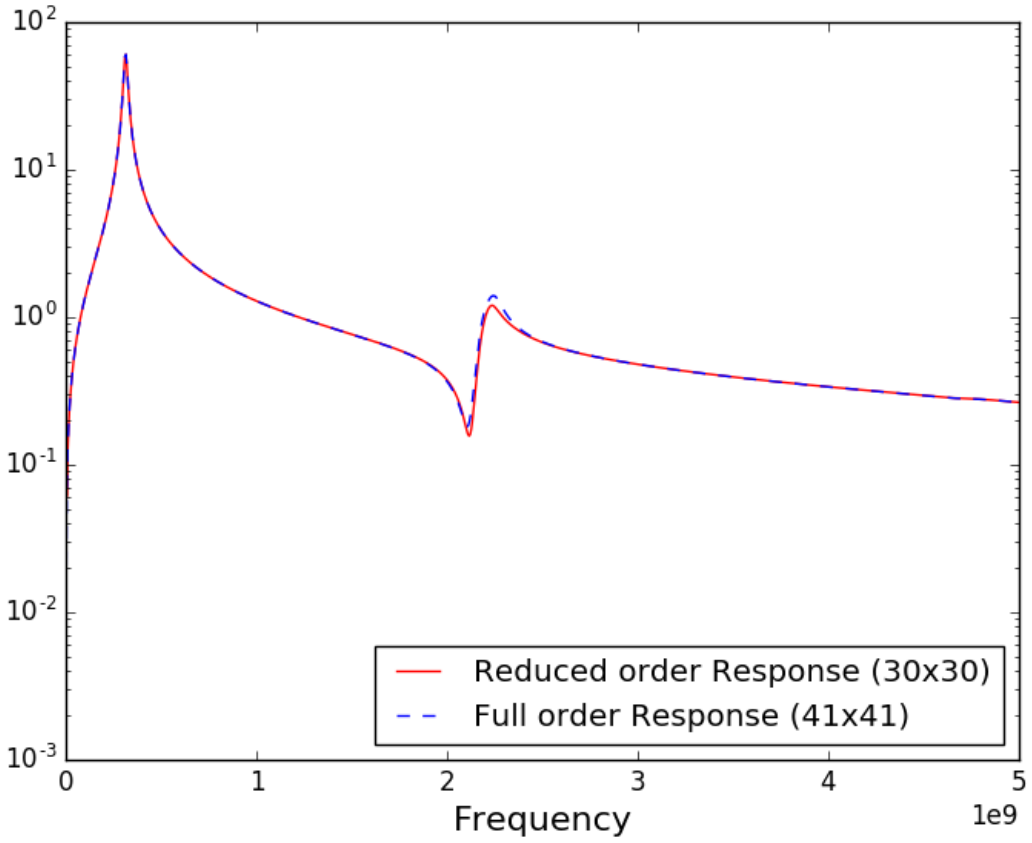

Figure 5.4: The large order system (41x41) reduced to (30x30) system and completely preserving original responsse

5.3 Summary

In this section, we have developed MNA formulation based on our topology to implement the SAPOR algorithm and presented several numerical experiments to demonstrate the efficiency of the SAPOR method. The advantages of this method will be more prominent as we implement this on larger scale systems.

CHAPTER 6

Conclusion

Macromodelling enables faster analysis in terms of runtime as it generates minimal behavioral counterparts coming from field simulation or direct estimations. A number of algorithms are available for extracting these macromodels. However, the main problem while developing a macromodel is guaranteeing passivity. As no passive element is able to produce energy, the representing models must have the same characteristic.

6.1 Summary

This thesis has studied the development in the field of passivity verification and enforcement. A broad description of all the techniques for passivity verification and enforcement has been reviewed and analyzed in this thesis. Ever since the concept of passivity has come to light, a diverse research endeavor has been attempted to achieve more and more efficient techniques on ensuring passivity in macromodels. A set of significant publications on passivity have been discussed in this thesis. We have presented illustrations to show the approaches and techniques. Different passivity enforcement algorithms have been demonstrated to comprehend passivity development. The purpose of this thesis is to provide a comprehensive analysis on the strengths and shortcomings of those methods and therefore it can play an important role for future research in this field.

In this thesis, at first we have developed a passivity verification and enforcement method by direct minimal modification of equivalent circuits. This method is valid for single-port systems only. Since Passivity can be verified by looking at the location of the system zeros in the Laplace-plane, we have also proposed some more passivity verification techniques based on computing the zeros by finding the local minima in the s-plane. The methods are i) computing real zeros based on local minima, ii) computing complex zeros based on local minima and iii) computing zeros of noisy transfer function by local minima. We have

presented another technique to extrapolate frequency domain response of macromodels to DC-point using 3-point data samples. Lastly, a Second Order Arnoldi Passive Order Reduction method has been implemented in Python and various numerical results have been presented to validate the implementation and accuracy of the method.

6.2 Significance of the Work

The passivity verification and enforcement method by direct minimal modification of equivalent circuits accurately validates the passivity of a macromodel without needing to construct Hamiltonian matrix, and overcomes the numerical difficulties associated in determining the imaginary eigenvalues of Hamiltonian matrices. All the zero detecting methods to assess passivity can successfully detect zeros of higher order systems with a varying range of zeros. The DC extrapolation method developed in Chapter 4 allows us to estimate the frequency response beneath the lowest available frequency sample of a model. Passivity is ensured in the extrapolated frequency response which facilitates transient simulation.

6.3 Future Work

There are few points highlighted here that can be topics of future research. The passivity verification and enforcement method developed in Chapter 2 is applicable to single port systems. The method can be further developed for multiport systems. This method is based on minimally changing the magnitude response. So, a topic of potential future work can be enforcing passivity by minimally changing both magnitude and phase responses. The cost effectiveness of the developed methods can be further compared with the existing commercially available passivity verification and enforcement methods.

In conclusion, this thesis can serve a significant role in the research field of passivity verification and enforcement. If these issues are addressed properly, more developments can be achieved for verifying and enforcing passivity of signal power integrity models.

Bibliography

[1] S. M and E. E. A., "Modeling of signal and power integrity in system on package applications," *IEEE International Symposium on Electromagnetic Compatibility*, pp. 1–6, 2007.

[2] R. Achar and M. S. Nakhla, "Simulation of high-speed interconnects," *Proceedings of the IEEE*, vol. 89, no. 5, pp. 693–728, 2001.

[3] W. T. Beyene and J. Schutt-Aine, "Interconnect simulation using order reduction and scattering parameters," in *Electronic Components amp; Technology Conference, 1998. 48th IEEE*. IEEE, 1998, pp. 627–631.

[4] W. T. Beyene and J. E. Schutt-Aine, "Efficient transient simulation of high-speed interconnects characterized by sampled data," *IEEE Transactions on Components, Packaging, and Manufacturing Technology: Part B*, vol. 21, no. 1, pp. 105–114, 1998.

[5] M. Elzinga, K. L. Virga, and J. L. Prince, "Improved global rational approximation macromodeling algorithm for networks characterized by frequency-sampled data," *IEEE Transactions on microwave theory and techniques*, vol. 48, no. 9, pp. 1461–1468, 2000.

[6] R. Achar, P. K. Gunupudi, M. Nakhla, and E. Chiprout, "Passive interconnect reduction algorithm for distributed/measured networks," *IEEE Transactions on Circuits and Systems II: Analog and Digital Signal Processing*, vol. 47, no. 4, pp. 287–301, 2000.

[7] E. A. Guillemin, *Synthesis of Passive Networks*. New York: Wiley, 1957.

[8] B. D. O. Anderson and S. Vongpanitlerd, *Network Analysis and Synthesis*. Englewood Cliffs, NJ: Prentice-Hall, 1973.

[9] M. R. Wohlers, *Lumped and Distributed Passive Networks*. New York: Academic, 1969.

[10] G. Raisbeck, "A definition of passive linear networks in terms of time and energy," *Journal of Applied Physics*, vol. 25, pp. 1510–1514, 1954.

[11] D. C. Youla, L. J. Castriota, and H. J. Carlin, "Bounded real scattering matrices and the foundations of linear passive network theory," *IRE Trans. Circuit Theory*, vol. CT-6, pp. 102–124, 1959.

[12] J. A. Resh, "A note concerning the n-port passivity criterion," *IEEE Trans. Circuit Theory*, vol. CT-13, pp. 238–239, 1966.

[13] Y. L. Kuo, "A note on the n-port passivity criterion," *IEEE Trans. Circuit Theory*, vol. CT-15, 1974.

[14] J. L. Wyatt, L. O. C. Jr., J. W. Gannett, I. C. Goknar, and D. N. Green, *Foundations of nonlinear network theory.* Univ. of California, Berkeley, 1978.

[15] S. Boyd and L. O. Chua, "On the passivity criterion for lti n-ports," in *Proc. IEEE Design, Automation and Test in Europe Conference and Exhibition (DATE)*, vol. 10, 1982, pp. 323–333.

[16] L. Fortuna, G. Nunnari, and A. Gallo, *Model order reduction techniques with applications in electrical engineering.* Springer Science & Business Media, 2012.

[17] R. Freund and P. Feldmann, "Efficient circuit analysis by pad e approximation via the lanczos process," in *Presentation at the workshop on Numerical Linear Algebra with Applications", Oberwolfach, Germany*, 1994.

[18] M. M. Alaybeyi, J. Y. Lee, and R. A. Rohrer, "Numerical integration algorithms and asymptotic waveform evaluation (awe)," in *Proceedings of the 1992 IEEE/ACM international conference on Computer-aided design.* IEEE Computer Society Press, 1992, pp. 76–79.

[19] D. L. Boley, "Krylov space methods on state-space control models," *Circuits, Systems and Signal Processing*, vol. 13, no. 6, pp. 733–758, 1994.

[20] Y. Saad, "Analysis of some krylov subspace approximations to the matrix exponential operator," *SIAM Journal on Numerical Analysis*, vol. 29, no. 1, pp. 209–228, 1992.

[21] L. T. Pillage and R. A. Rohrer, "Asymptotic waveform evaluation for timing analysis," *IEEE Trans. on CAD*, vol. 9, 1990.

[22] W. E. Arnoldi, "The principle of minimized iterations in the solution of the matrix eigenvalue problem," *Quart. Appli. Math*, vol. 9, 1951.

[23] A. Odabasioglu, M. Celik, and L. Pileggii, "Prima: passive reduced order interconnect macromodeling algorithm," *Tech. Dig. 1997 IEEE/ACM ICCAD*, 1997.

[24] Y. Liu, L. T. Pileggi, and A. J. Strojwas, "Model order-reduction of rc (l) interconnect including variational analysis," in *Proceedings of the 36th annual ACM/IEEE Design Automation Conference*. ACM, 1999, pp. 201–206.

[25] L. Daniel, O. C. Siong, L. S. Chay, K. H. Lee, and J. White, "A multiparameter moment-matching model-reduction approach for generating geometrically parameterized interconnect performance models," *IEEE Transactions on Computer-Aided Design of Integrated Circuits and Systems*, vol. 23, no. 5, pp. 678–693, 2004.

[26] N. Mi, S. X.-D. Tan, Y. Cai, and X. Hong, "Fast variational analysis of on-chip power grids by stochastic extended krylov subspace method," *IEEE Transactions on Computer-Aided Design of Integrated Circuits and Systems*, vol. 27, no. 11, pp. 1996–2006, 2008.

[27] F. Ferranti, G. Antonini, T. Dhaene, and L. Knockaert, "Passivity-preserving parameterized model order reduction for peec based full wave analysis," in *IEEE 14th Workshop of Signal Propagation on Interconnects (SPI)*, 2010, pp. 65–68.

[28] B. Gustavsen and A. Semlyen, "Rational approximation of frequency domain responses by vector fitting," *IEEE Transactions on power delivery*, vol. 14, no. 3, pp. 1052–1061, 1999.

[29] D. Deschrijver, B. Haegeman, and T. Dhaene, "Orthonormal vector fitting: A robust macromodeling tool for rational approximation of frequency domain responses," *IEEE Transactions on Advanced Packaging*, vol. 18, pp. 216–225, May 2007.

[30] D. Deschrijver, M. Mrozowski, T. Dhaene, and D. D. Zutter, "Macromodeling of multiport systems using a fast implementation of the vector fitting method," *IEEE Microwave and Wireless Components Letters*, vol. 18, pp. 383–385, June 2008.

[31] S. Grivet-Talocia, S. Olivadesei, and P. Triverio, "A compression strategy for rational macromodeling of large interconnect structures," in *Conference on Electrical Performance of Electronic Packaging and Systems (EPEPS)*, San Jose, CA, Oct. 23–26, 2011, pp. 53–56.

[32] A. Semlyen and B. Gustavsen, "Vector fitting by pole relocation for the state equation approximation of nonrational transfer matrices," *Circuit Syst. Signal Process*, vol. 19, pp. 549–566, 2000.

[33] B. Gustavsen and A. Semlyen, "A robust approach for system identification in the frequency domain," *IEEE Trans. Power Delivery.*, vol. 19, pp. 1167–1173, 2004.

[34] A. Mayo and A. Antoulas, "A framework for the solution of the generalized realization problem," *Linear algebra and its applications*, vol. 425, no. 2, pp. 634–662, 2007.

[35] S. Lefteriu and A. C. Antoulas, "A new approach to modeling multiport systems from frequency-domain data," *IEEE Transactions on Computer-Aided Design of Integrated Circuits and Systems*, vol. 29, no. 1, pp. 14–27, 2010.

[36] Y. Wang, C.-U. Lei, G. K. Pang, and N. Wong, "Mfti: Matrix-format tangential interpolation for modeling multi-port systems," in *Proceedings of the 47th Design Automation Conference*. ACM, 2010, pp. 683–686.

[37] M. Kabir and R. Khazaka, "Macromodeling of distributed networks from frequency-domain data using the loewner matrix approach," *IEEE Transactions on Microwave Theory and Techniques*, vol. 60, no. 12, pp. 3927–3938, 2012.

[38] M. Kabir, R. Khazaka, R. Achar, and M. Nakhla, "Loewner-matrix based efficient algorithm for frequency sweep of high-speed modules," in *Electrical Performance of Electronic Packaging and Systems (EPEPS), 2012 IEEE 21st Conference on*, 2012, pp. 185–188.

[39] M. Kabir and R. Khazaka, "Parametric macromodeling of high-speed modules from frequency-domain data using loewner matrix based method," in *Microwave Symposium Digest (IMS), 2013 IEEE MTT-S International*. IEEE, 2013, pp. 1–4.

[40] D. Saraswat, R. Achar, and M. Nakhla, "Enforcing passivity for rational function based macromodels of tabulated data," in *Proc. IEEE Electrical Performance of Electronic Packaging*, 2003, pp. 295–298.

[41] S. P. Boyd, L. El Ghaoui, E. Feron, and V. Balakrishnan, *Linear matrix inequalities in system and control theory*. SIAM, 1994, vol. 15.

[42] S. Grivet-Talocia, "Passivity enforcement via perturbation of hamiltonian matrices," *IEEE Transactions on Circuits and Systems I: Regular Papers*, vol. 51, no. 9, pp. 1755–1769, 2004.

[43] S. Boyd, V. Balakrishnan, and P. Kabamba, "A bisection method for computing the h norm of a transfer matrix and related problems," *Mathematics of Control, Signals and Systems*, vol. 2, no. 3, pp. 207–219, 1989.

[44] E. D. Campbell, A. Morales, and S. Agili, ""A simple method for restoring passivity in s-parameters using singular value decomposition"," *Digest of Technical Papers ICCE*, pp. 219–220, 2010.

[45] D. Saraswat, R. Achar, and M. Nakhla, "Fast passivity verification and enforcement via reciprocal systems for interconnects with large order macromodels," in *IEEE Trans. VLSI Syst.*, vol. 15, 2007, pp. 48–59.

[46] S. Grivet-Talocia, "An adaptive sampling technique for passivity characterizationand enforcement of large interconnect macromodels," *IEEE Transactions on Advanced Packaging*, vol. 30, pp. 226–237, May 2007.

[47] Y. Liu and N. Wong, "Fast sweeping methods for checking passivity of descriptor systems," in *IEEE Asia-Pacific Conference on Circuits and Systems (APC-CAS)*, 2008, pp. 1794–1797.

[48] Z. Zhang, C.-U. Lei, and N. Wong, "Ghm: A generalized hamiltonian method for passivity test of impedance/admittance descriptor systems," in *Proceedings of the 2009 International Conference on Computer-Aided Design*. ACM, 2009, pp. 767–773.

[49] Z. Zhang and N. Wong, "Passivity test of immittance descriptor systems based on generalized hamiltonian methods," *IEEE Transactions on Circuits and Systems II: Express Briefs*, vol. 57, no. 1, pp. 61–65, 2010.

[50] ——, "Passivity check of s-parameter descriptor systems via sparameter generalized hamiltonian methods," *IEEE Transactions on Advanced Packaging*, vol. 33, no. 4, pp. 1034–1042, 2010.

[51] C. P. Coelho, J. Phillips, and L. M. Silveira, "A convex programming approach for generating guaranteed passive approximations to tabulated frequency-data," *IEEE Transactions on Computer-Aided Design of Integrated Circuits and Systems*, vol. 23, pp. 293–301, February 2004.

[52] S. Grivet-Talocia and A. Ubolli, "On the generation of large passivemacromodels for complex interconnect structures," *IEEE Transactions on Advanced Packaging*, vol. 29, pp. 39–54, February 2006.

[53] B. Gustavsen, "Fast passivity enforcement for pole-residue models by perturbation of residue matrix eigenvalues," *IEEE Trans. Power Delivery.*, vol. 23, pp. 2278–2285, October 2008.

[54] S. Grivet-Talocia and A. Ubolli, "Passivity enforcement with relative error control," *IEEE Trans. Microwave Theory and Techniques*, vol. 55, pp. 2374–2383, November 2007.

[55] T. Dhaene, D. Deschrijver, and N. Stevens, "Efficient algorithm for passivity enforcement of s-parameter-based macromodels," *IEEE Trans. Microwave Theory and Techniques*, vol. 57, pp. 415–420, February 2009.

[56] D. Deschrijver and T. Dhaene, "Fast passivity enforcement of s-parameter macromodels by pole perturbation," *IEEE Trans. Microwave Theory and Techniques*, vol. 57, pp. 620–626, March 2009.

[57] T. Wang and Z. Ye, "Robust passive macro-model generation with local compensation," *IEEE Trans. Microwave Theory and Techniques*, vol. 60, 2012.

[58] S. Boyd and L. Vandenberghe, *Convex optimization*. Cambridge university press, 2004.

[59] G. C. Calafiore, A. Chinea, and S. Grivet-Talocia, "Subgradient techniques for passivity enforcement of linear device and interconnect macromodels," *IEEE Trans. Microwave Theory and Techniques*, vol. 60, pp. 2990–3003, October 2012.

[60] A. Semlyen and B. Gustavsen, "A half-size singularity test matrix for fast and realiable passivity assessment of rational models," *IEEE Trans. Power Delivery.*, vol. 24, pp. 345–351, January 2009.

[61] B. Gustavsen and A. Semlyen, "Fast passivity assessment for s-parameter rational models via a half-size test matrix," *IEEE Trans. Microwave Theory and Techniques*, vol. 56, pp. 2701–2708, December 2008.

[62] B. Gustavsen, "Fast passivity assessment of admittance parameter macromodels by a half-size singularity test matrix," in *Proc. Signal Propagation on Interconnects*, 2008, pp. 1–4.

[63] Z. Ye, L. M. Silveira, and J. R. Phillips, "Fast and reliable passivity assessment and enforcement with extended hamiltonian pencil," in *International Conference on Computer Aided Design*, 2009, pp. 774–778.

[64] ——, "Extended hamiltonian pencil for passivity assessment and enforcement for s-parameter systems," in *Proc. IEEE Design, Automation and Test in Europe Conference and Exhibition (DATE)*, 2010, pp. 1148–1152.

[65] L. Gobbato, A. Chinea, and S. Grivet-Talocia, "A parallel hamiltonian eigensolver for passivity characterization and enforcement of large interconnect macromodels," in *Proc. IEEE Design, Automation and Test in Europe Conference and Exhibition (DATE)*, 2011, pp. 1–6.

[66] C. S. Saunders and M. B. Steer, "Passivity enforcement for admittance models of distributed networks using an inverse eigenvalue method," *IEEE Trans. Microwave Theory and Techniques*, vol. 60, pp. 8–20, 2011.

[67] Y.-C. Wang, S. Yin, M. Jun, X. Li, L. T. Pileggi, T. Mukherjee, and R. Negi, "Accurate passivity-enforced macromodeling for rf circuits via iterative zero/pole update based on measurement data," in *Proc. IEEE Design Automation Conference(ASP-DAC)*, 2015, pp. 441–446.

[68] C. S. Saunders, J. Hu, C. E. Christoffersen, and M. B. Steer, "Inverse singular value method for enforcing passivity in reduced-order models of distributed structures for

transient and steady-state simulation," *IEEE Trans. Microwave Theory and Techniques*, vol. 59, pp. 837–847, 2011.

[69] A. Chakrabarti, S. Agili, A. Morales, and M. Resso, "An efficient and simple algorithm to restore passivity for measured s-parameters data," in *2015 International Symposium on Consumer Electronics (ISCE)*. IEEE, 2015, pp. 1–2.

[70] M. Zhang and Z. Ye, "Tackling close-to-band passivity violations in passive macromodeling," in *Proc. IEEE Design Automation Conference(ASP-DAC)*, 2014, pp. 768–773.

[71] A. Ubolli, S. Grivet-Talocia, M. Bandinu, and A. Chinea, "Sensitivity-based weighting for passivity enforcement of linear macromodels in power integrity applications," in *Proc. IEEE Design, Automation and Test in Europe Conference and Exhibition (DATE)*, 2014, pp. 1–6.

[72] Z. Mahmood, S. Grivet-Talocia, A. Chinea, G. C. Calafiore, and L. Daniel, "Efficient localization methods for passivity enforcement of linear dynamical models," *IEEE Transactions on Computer-Aided Design of Integrated Circuits and Systems*, vol. 33, no. 9, pp. 1328–1341, 2014.

[73] Z. Mahmood, S. Grivet-Talocia, G. C. Calafiore, and L. Daniel, "Optimal passivity enforcement of state-space models via localization methods," 2014.

[74] L. P. Ihlenfeld, G. H. Oliveira, and M. R. Sans, "A data passivity-enforcement preprocessing approach to multiport system modeling," *IEEE Transactions on Power Delivery*, vol. 31, no. 3, pp. 1351–1359, 2016.

[75] Z. Ye, T. Wang, and Y. Li, "Domain-alternated optimization for passive macromodeling," *IEEE Transactions on Very Large Scale Integration (VLSI) Systems*, vol. 23, no. 10, pp. 2244–2255, 2015.

[76] Y. Su, J. Wang, X. Zeng, Z. Bai, C. Chiang, and D. Zhou, "Sapor: Second-order arnoldi method for passive order reduction of rcs circuits," in *Proceedings of the 2004 IEEE/ACM International conference on Computer-aided design*. IEEE Computer Society, 2004, pp. 74–79.

[77] A. Zadehgol, "A semi-analytic and cellular approach to rational system characterization through equivalent circuits," *International Journal of Numerical Modelling: Electronic Networks, Devices and Fields*, 2015.

[78] Y. Wang, Z. Zhang, C.-K. Koh, G. Shi, G. K. Pang, and N. Wong, "Passivity enforcement for descriptor systems via matrix pencil perturbation," *IEEE Transactions on Computer-Aided Design of Integrated Circuits and Systems*, vol. 31, no. 4, pp. 532–545, 2012.

[79] S. Grivet-Talocia and B. Gustavsen, *Passive macromodeling: Theory and applications*. John Wiley & Sons, 2015, vol. 239.

[80] B. Kouvaritakis and A. MacFarlane, "Geometric approach to analysis and synthesis of system zeros part 1. square systems," *International Journal of Control*, vol. 23, no. 2, pp. 149–166, 1976.

[81] P. Misra, G. Gu, and P. Van Dooren, "Characterization and computation of transmission zeros of singular multivariable systems," in *Decision and Control, 1990., Proceedings of the 29th IEEE Conference on*. IEEE, 1990, pp. 279–284.

[82] C.-T. Chen, *Linear system theory and design*. Oxford University Press, Inc., 1995.

[83] C. Sanathanan and J. Koerner, "Transfer function synthesis as a ratio of two complex polynomials," *IEEE transactions on automatic control*, vol. 8, no. 1, pp. 56–58, 1963.

[84] F. Callier and C. Desoer, "An algebra of transfer functions for distributed linear time-invariant systems," *IEEE Transactions on Circuits and Systems*, vol. 25, no. 9, pp. 651–662, 1978.

[85] A. Emami-Naeini and P. Van Dooren, "Computation of zeros of linear multivariable systems," *Automatica*, vol. 18, no. 4, pp. 415–430, 1982.

[86] A. Zadehgol, "A frequency-independent and parallel algorithm for computing the zeros of strictly proper rational transfer functions," *Applied Mathematics and Computation*, vol. 274, pp. 229–236, 2016.

[87] N. Yamin and A. Zadehgol, "A novel algorithm for computing the zeros of transfer functions by local minima," in *Conference on Electrical Performance of Electronic Packaging and Systems (EPEPS)*, San Diego, CA, Oct. 23–26, 2016.

[88] W. Kim, J.-H. Kim, D. Oh, and C. Yuan, "S-parameters based transmission line modeling with accurate low-frequency response," in *Electrical Performance of Electronic Packaging, 2006 IEEE*. IEEE, 2006, pp. 79–82.

[89] D. Gope, A. Ruehli, and V. Jandhyala, "Solving low-frequency em-ckt problems using the peec method," *IEEE Transactions on Advanced Packaging*, vol. 30, no. 2, pp. 313–320, 2007.

[90] V. Avula and A. Zadehgol, "Pole residue equivalent system solver (press)," in *Signal and Power Integrity (SPI), 2016 IEEE 20th Workshop on*. IEEE, 2016, pp. 1–4.

[91] N. Yamin and A. Zadehgol, "Verification and enforcement of passivity through direct minimal modification of equivalent circuits," in *Electromagnetic Compatibility-EMC EUROPE, 2016 International Symposium on*. IEEE, 2016, pp. 756–759.

[92] Z. Bai and Y. Su, "Soar: A second-order arnoldi method for the solution of the quadratic eigenvalue problem," *SIAM Journal on Matrix Analysis and Applications*, vol. 26, no. 3, pp. 640–659, 2005.